JCI insight
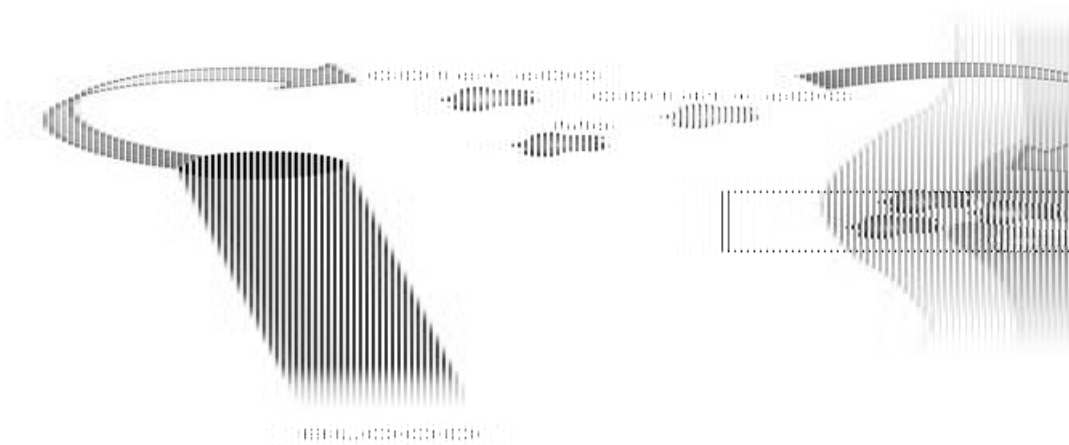
NLRC4 -mediated activation of CD1c+ dendritic cells contributes to perpetuation of synovitis in rheumatoid arthritis

Cristina Delgado-Arévalo, … , Isidoro González-Álvaro, Enrique Martin-Gayo

Research In-Press Preview Cell biology

Graphical abstract

Find the latest version:

https://jci.me/152886/pdf

NLRC4 -mediated activation of CD1c+ dendritic cells

contributes to perpetuation of synovitis in rheumatoid arthritis

Cristina Delgado-Arévalo[1]*, Marta Calvet-Mirabent[1]*, Ana Triguero-Martínez[2]*, Enrique Vázquez de Luis[3], Alberto Benguría-Filippini[3], Raquel Largo[4], Diego Calzada-Fraile[1,5], Olga Popova[1], Ildefonso Sánchez-Cerrillo[1], Ilya Tsukalov[1], Roberto Moreno-Vellisca[3], Hortensia de la Fuente[1,5], Gabriel Herrero-Beaumont[4], Almudena Ramiro[6], Francisco Sánchez-Madrid[1,5,6], Santos Castañeda[2,7], Ana Dopazo[3,5], Isidoro González Álvaro[2Ψ], Enrique Martin-Gayo[1,8Ψ#]

*These authors contributed equally to the study

ΨThese senior authors equally led and supervised the study.

[1]Immunology Unit from Hospital Universitario La Princesa, Medicine Faculty, Universidad Autónoma de Madrid, Instituto Investigación Sanitaria-Princesa IIS-IP; [2]Rheumatology Department from Hospital Universitario La Princesa. Instituto de Investigación Sanitaria-Princesa IIS-IP; [3]Genomic Unit, Centro Nacional de Investigaciones Cardiovasculares; [4]Bone and Joint Research Unit, Rheumatology Service, IIS Fundación Jiménez Díaz; [5]CIBER Cardiovascular, [6]Biology Laboratory, Centro Nacional de Investigaciones Cardiovasculares; [7]Cátedra UAM-Roche, EPID-Future, Department of Medicine, Universidad Autónoma de Madrid (UAM); [8]CIBER Enfermedades Infecciosas

 # Corresponding author:

Enrique Martin-Gayo Ph.D. Assistant Professor, Universidad Autónoma de Madrid; Immunology Unit, Hospital de la Princesa; Calle de Diego de León, 62, 28006 Madrid, Spain, E-mail: enrique.martin@uam.es

CONFLICT OF INTEREST STATEMENT

ABSTRACT

The individual contribution of specific myeloid subsets such as $CD1c^+$ conventional dendritic cells (cDC) to perpetuation of Rheumatoid Arthritis (RA) pathology remains unclear. In addition, the specific innate sensors driving pathogenic activation of $CD1c^+$ cDCs in RA patients and their functional implications have not been characterized. Here, we assessed phenotypical, transcriptional and functional characteristics of $CD1c^+$ and $CD141^+$ cDCs and monocytes from the blood and synovial fluid of RA patients. Increased levels of CCR2 and the IgG receptor CD64 on circulating $CD1c^+$ cDC associated with the presence of this DC subset in the synovial membrane in RA patients. Moreover, synovial $CD1c^+$ cDCs are characterized by increased expression of proinflammatory cytokines and high abilities to induce pathogenic $IFN\gamma^+IL-17^+$ $CD4^+$ T cells in vitro. Finally, we identified the crosstalk between Fcγ Receptors and NLRC4 as a new potential molecular mechanism mediating pathogenic activation, CD64 upregulation and functional specialization of $CD1c^+$ cDCs in response to dsDNA-IgG in RA patients.

Keywords: Rheumatoid arthritis, dendritic cell, Th1/Th17, Fc-receptor, inflammasome, NLRC4.

INTRODUCTION

Rheumatoid arthritis (RA) pathogenesis is a multifactorial process that involves the crosstalk between multiple adaptive and innate immune cell subsets leading to chronic synovitis and the progressive destruction of joint cartilage and bone tissue. Altered adaptive immune responses in patients with active RA disease mediated by autoantibody-producing B cells (1-3), Th1 and Th17 CD4^{+} T cells (4, 5) and activated cytotoxic CD8^{+} T cells (6) have been well characterized. However, less is known about the contribution of specific innate cell populations to perpetuate chronic inflammation and the induction of pathogenic CD4^{+} T cells able to produce both IL-17 and IFNγ (known as Th1/Th17 cells), a T cell subset which is enriched in synovial fluid (SF) of RA patients (7) and has been linked to severity of multiple autoimmune disorders (8-10). In this regard, deregulation of myeloid cells such as monocytes (Mo) and dendritic cells (DC) can lead to the development of autoimmunity (11, 12). However, the heterogeneity of Mo and DC lineages has made difficult to fully understand the contribution of individual cell subsets to RA pathology. Several studies have reported alterations in Mo subset phenotype and function in the peripheral blood (PB) and SF from RA patients (13-15) and their participation in the erosion of juxta-articular bone (14, 16). In contrast, less is known about the contribution of different subtypes of DCs to RA immuno-pathology (17).

DCs can be divided into two main subgroups, conventional (cDC) and plasmacytoid (pDC) DCs, with different functional specializations (18, 19). pDCs physiologically mediate type I IFN responses in the context of viral infections (20) but have also been involved in autoimmune disorders such as systemic lupus erythematosus and psoriasis (20). In addition, pDCs appear to play a tolerogenic role on RA joint inflammation (21, 22). In contrast, cDCs can be subdivided into CD141^{+} and CD1c^{+} cDCs with differential abilities to efficiently activate CD8^{+} and CD4^{+} T cell responses, respectively (23, 24).

Frequencies of both CD141$^+$ and CD1c$^+$ cDCs have been reported to be reduced in the PB and enriched in the SF of RA patients. Moreover, CD141$^+$ and CD1c$^+$ cDCs in SF of RA individuals can induce IFNγ$^+$ and TNFα$^+$ CD4$^+$ T cells (22, 25) or IL-17 secretion by T cells in vitro (26) in individual studies. However, potential differences in functional capacities of both cDC subsets and in Mo from RA patients to induce pathogenic IL-17$^+$ IFNγ$^+$ T cells have not been directly addressed. In addition, the molecular mechanisms specifically affecting phenotypical and functional properties of CD1c$^+$ cDCs in RA patients and the functional implications of these alterations have not been characterized. Previous Genome Wide Association Studies (GWAS) identified genetic variations related to class II-HLA, Tumor Necrosis Factor (TNF)-α, Fc-receptor, toll-like receptor (TLR) and nucleic acid sensing pathways that are associated with increased risk of developing RA (27-30). Several studies have also suggested that recognition of endogenous DNA and RNA as DAMPs by nucleic-acid sensors might induce innate responses that contribute to the development of autoimmunity, including RA (31). In addition, activation of alternative innate pathways such as the NLRP3 inflammasome has been proposed as a pathogenic activation mechanism of Mo in RA (32, 33). However, it is unknown whether common or different innate sensors may differentially mediate pathogenic activation of CD1c$^+$ cDC and other myeloid cells in RA. In fact, the most accepted treatments nowadays are based on the blockade of inflammatory cytokines or their receptors, which are not always effective (34, 35). Therefore, it is critical to identify innate sensors that might be specifically mediating pathogenic activation in different myeloid subsets in RA, to design more targeted and effective therapies.

The objective of our study was to specifically investigate the contribution of CD1c$^+$ cDC to chronic disease perpetuation and the mechanism of pathogenic activation of these cells in RA. Our phenotypical, transcriptional and functional analysis identified CD64 and

CCR2 as markers of activated migratory CD1c$^+$ cDCs enriched in the inflamed joint from RA patients, which are selectively restored in the PB after treatment initiation and reduction of clinical severity. In addition, CD1c$^+$ cDCs from the SF of RA patients are characterized by preferential expression of IL1β, IL-8 and CCL3 and by higher functional abilities to induce pathogenic IL-17$^+$ IFNγ$^+$ T cell responses in vitro compared to other synovial myeloid subsets. Interestingly, inflammatory and functional RA-like properties could be induced in vitro on CD1c$^+$ cDC by incubation with dsDNA-IgG complexes. Remarkably, we have identified the NLRC4 as a new sensor required for Fc-γ-Receptor mediated detection of dsDNA-IgG complexes, thereby inducing Caspase 1-dependent inflammasome activation of CD1c$^+$ cDC subset. Collectively, our translational study provides new evidence of active contribution of CD1c$^+$ cDC to RA disease progression and identifies new therapeutic target candidates that might be useful for novel targeted therapies for RA.

RESULTS

Frequencies of CD64$^+$ CD1c$^+$ cDCs in the blood are restored in treated RA patients with reduced disease activity

Proportions of CD1c$^+$ and CD141$^+$ cDC and to a lower extent pDC, were markedly reduced in the PB of thirty one RA patients recruited prior to initiating treatment and compared to thirty healthy controls (HC) including 13 age and sex matched individuals (Supplemental Figure 1A-B, Supplemental Table1), in line with previous studies (25). In contrast, frequencies of classical (C), transitional (T) and non-classical (NC) monocytes (Mo) were not significantly different between these two cohorts (Supplemental Figure 1B). Of these populations, T-Mo and both CD1c$^+$ and CD141$^+$ cDC subsets were more significantly enriched in SF from RA patients obtained during flares despite they were receiving treatment (Supplemental Figure 1B; Supplemental Table 2). We next analyzed the evolution of proportions of circulating cDC and Mo subsets in n=14 RA patients in a longitudinal follow up study after treatment for either 1 or 2 years (Supplemental Table 3). We observed that, in treated RA patients experiencing improvement of clinical values over time, such as lower number of swollen joints and lower disease activity assessed by DAS28-ESR score (Figure 1A), proportions of circulating CD1c$^+$ cDC were more significantly recovered (nominal p=0.0067; FDR-corrected p=0.0335) (Figure 1B). Proportions of CD1c$^+$ cDC were not significantly associated with age on the RA and HC cohorts (Supplemental Figure 1C). In contrast, frequencies of circulating Mo and CD141$^+$ cDC were not significantly affected in these treated individuals (Supplemental Figure 1D). Therefore, CD1c$^+$ cDC might be differentially altered in RA patients. A phenotypical analysis of circulating myeloid subsets showed a non-significant trend to increased expression of CD40 on cDC (Figure 1C). However, expression of CD40 was significantly upregulated in CD1c$^+$ cDCs from SF and it also tended to be increased in

CD141$^+$ cDCs from this location (Figure 1C). In addition, we also identified a trend of increased CD86 levels in circulating CD1c$^+$ and CD141$^+$ cDCs and NC-Mo, which was not observed in pDCs or in SF Mo subsets from RA patients (Supplemental Figure 2A-C). Remarkably, PB and SF CD1c$^+$ but not CD141$^+$ cDCs showed significantly higher expression of CD64 (Figure 1C). Proportions of CD64$^+$ cells in CD1c$^+$ cDC were not significantly associated with higher disease activity (Supplemental Figure 2D). Interestingly, CD64 expression levels tended to remain upregulated in CD1c$^+$ cDCs even in treated RA patients (Figure 1D). In contrast, CD64 expression was basally the highest in C-Mo but did not significantly increase in circulating cells. On the other hand, CD64 was significantly elevated on T- and NC-Mo from SF (Supplemental Figure 2B) in agreement with previous studies (36). In addition, no alterations in expression of alternative Fc-Receptors such as CD16 on CD1c$^+$ on CD141$^+$ cDCs, neither on Mo were detected, while pDC displayed a mild increase in RA patients (Figure 1C and Supplemental Figure 2A-B). Therefore, differential maturation programs might be taking place in CD1c$^+$ cDC compared to CD141$^+$ cDC and Mo. Together, our data indicate that CD1c$^+$ cDCs from RA individuals are preferentially restored after treatment initiation and are characterized by the differential expression of the cell surface marker CD64, suggesting a significant contribution of this DC subset to the perpetuation of RA pathology.

Specific transcriptional profiles of innate activation in CD1c$^+$ cDCs in RA patients

Next, differential transcriptional patterns of circulating CD1c$^+$ and CD141$^+$ cDCs and Mo from the PB of n=4 RA patients and n=4 HC were characterized. Principal Component Analysis (PCA) of detected genes suggested that each cell subset in RA was transcriptionally different from its corresponding HC (Supplemental Figure 3). A

comparative gene expression analysis considering FDR-corrected significant p values and changes in Log2 fold change of expression over 1.5 or less than -1.5, identified a total of 784, 1078 and 781 significant differentially expressed genes (DEG) in Mo, CD1c$^+$ and CD141$^+$ cDCs from RA compared to HC, respectively (Figure 2A; Supplemental Table 4). Importantly, a portion of 251 and 224 DEG from CD1c$^+$ cDCs overlapped with those present in CD141$^+$ cDCs and with Mo, respectively (Figure 2A), while 402 DEG were exclusively detected in CD1c$^+$ cDC. Low level of DEG overlap (29 genes) was observed between Mo and CD141$^+$ cDC (Figure 2A). Ingenuity Pathway Analysis (IPA) identified differences in relevant pathways associated with innate activation enriched in DEG in the three myeloid subsets from RA patients (Figure 2B; Supplemental Table 5). Interestingly, genes related to TLR stimulation, pyroptosis, the inflammasome, Fcγ and Fcε receptor signaling, activation of PRR, signaling of inflammatory cytokines such as IL-1β, IL-6, IL-8 and fMLP (N-Formyl-methionine-leucyl-phenylalanine) were more significantly predicted to be affected in CD1c$^+$ cDCs compared to other myeloid subsets from PB of RA individuals (Figure 2B, Supplemental Table 5). Paradoxically, some inflammatory cytokine signaling pathways appeared to be mainly downregulated in these cells from PB in RA patients (Figure 2B), but some components of these and other innate pathways such as TLR and FcR remained upregulated (Supplemental Table 4, Supplemental Figure 4A-C). Importantly, these predicted pathways on CD1c$^+$ cDC were highly interconnected and appeared to share a significant number of DEG (Figure 2C, left). The pathways sharing the highest number of DEG were TLR with IL-1 and pyroptosis, and between pyroptosis and the inflammasome and IL-1 and IL-6 pathways (Figure 2C, right).

To better understand how transcriptional profiles of circulating CD1c$^+$ cDC were related to the patterns present in the same cell subsets infiltrated in SF from RA individuals, we performed an additional RNA-seq analysis of n=3 RA and n=3 Calcium Pyrophosphate

Deposition (CPPD)-crystal associated arthritis patients (Supplemental Table 2). Given the low number and the similar inflammatory nature of both types of SF samples used, we considered nominal $p<0.05$ as significance cut-off to identify DEG for each myeloid subset from RA (Supplemental Table 6). In these analyses, a higher but limited overlap of DEG was observed between CD1c$^+$ cDCs and Mo, compared to CD141$^+$ cDCs (Supplemental Figure 5). When the lists of DEG obtained for each cell subset in blood and SF were compared (Supplemental Tables 4 and 6), 73 overlapping DEG in CD1c$^+$ cDCs were detected (Figure 2D), which were also enriched in TLR and IL-1 related pathways in CD1c$^+$ cDCs from both blood and SF in RA patients (Figure 2E). However, non-overlapping transcriptional patterns in CD1c+ cDC from SF and PB more significantly predicted alterations in the IL-1 pathway (Figure 2E), indicating different components of the pathway enriched in cells from these two locations. Therefore, CD1c$^+$ cDCs from the PB and SF of RA patients are characterized by specific transcriptional signatures associated to TLR, inflammasome and proinflammatory cytokines.

Identification of CCR2 as a marker for migratory CD64^{Hi} CD1c$^+$ cDCs in RA patients

We subsequently analyzed the expression of inflammatory cytokines downstream the TLR and inflammasome pathways in myeloid subsets from RA individuals. Interestingly, RNA-seq data and RT-qPCR validation indicated that expression of proinflammatory cytokines such as IL-1β, IL-8 and MIP1α (CCL3) was downregulated in circulating CD1c$^+$ cDC, CD141$^+$ cDC and Mo from RA patients compared to HC (Figure 3A-B; Supplemental Figure 6A). These data may indicate selective migration of activated inflammatory cDCs and Mo from the blood to other anatomical locations in RA patients, such as the synovial membrane. Thus, we analyzed the transcriptional expression of chemokine receptors that might be differentially expressed in circulating cDC subsets and

Mo from RA patients in our RNA-seq dataset. As shown in Figure 3C-D, we observed significantly higher expression of CCR2 in CD1c$^+$ cDCs. These findings were accompanied by confirmation of increased XCR1 expression CD141$^+$ cDCs (Figure 3C) reported in a previous study (25). In addition, we also detected significant changes on CXCR4, CX3CR1 and CCR6 transcriptional levels on circulating CD1c$^+$ cDCs from RA individuals, but we focused on CCR2 since it has been recently involved to migration of Mo to synovium (37, 38) (Figure 3C). Importantly, FACS analysis indicated that proportions of CD1c$^+$ cDCs expressing higher surface levels of CCR2 were increased in RA patients compared to HC (Figure 3D). Interestingly, CCR2^{Hi} CD1c$^+$ cDCs also expressed significantly higher levels of CD64 (Figure 3E), indicating that these cells represented a subpopulation migrating from the blood enriched in activated cells. Supporting this possibility, higher proportions of CCR2$^+$ cells were also found in Mo and CD1c$^+$ cDC infiltrated in the SF from RA subjects (Figure 3F), in which high CD64 expression was previously observed (Figure 1C). Together, our data indicate that CCR2 is an additional marker defining a subpopulation of migratory CD1c$^+$ cDC enriched for CD64 expression in the blood and selectively enriched in the SF from RA patients.

Inflammatory CD1c$^+$ cDCs present in SF from RA patients efficiently activate pathogenic IFNγ$^+$ IL-17$^+$ T cells

Recruitment of CD1c$^+$ cDC to the SF suggested that these cells could potentially contribute to the joint inflammation in RA patients. Supporting this possibility, RNA-seq and RT-qPCR analyses confirmed that expression of IL-1β, IL-8 and MIP1α tended to be elevated in Mo and CD1c$^+$ cDCs but not CD141$^+$ cells from SF samples from RA patients compared to alternative synovial myeloid cells from individuals suffering CPPD crystal-associated arthropathy (Figure 4A; Supplemental Figure 6A). At a functional

level, from the three synovial myeloid cell subsets isolated ex vivo from RA-SF samples, Mo and CD1c$^+$ cDC were both capable of inducing proliferation of allogeneic CD4$^+$ T cells and the activation of a significant portion of these T cells acquiring a Th1-like IFNγ$^+$ IL-17$^-$ phenotype (Supplemental Figure 6B-C). In addition, Mo and CD1c$^+$ cDC also tended to support proliferation of CD8$^+$ T cells and their activation leading to the induction of cytotoxic IFNγ$^+$ CD107a$^+$ cells in vitro (Supplemental Figure 6D). However, inflammatory patterns of SF CD1c$^+$ cDCs and Mo from RA patients were associated with a more efficient induction of IL-17$^+$ CD4$^+$ T cells, compared to CD141$^+$ cDCs (Figure 4B-C, Supplemental Figure 6B). Importantly, higher frequencies of pathogenic IFNγ$^+$ IL-17$^+$ T cells included within IL-17$^+$ cells were more significantly induced by SF CD1c$^+$ cDCs (Figure 4B-C, Supplemental Figure 6B). Moreover, we observed CD1c$^+$ cDCs in close proximity to IL-17$^+$ T cells in the synovial membrane from RA patients presenting advanced joint destruction, some of which displayed a pathogenic IFNγ$^+$ IL17$^+$ phenotype (Figure 4D, Supplemental Figure 6E). Thus, these data indicate that CD1c$^+$ cDCs may actively contribute to inflammatory environment and to activating pathogenic Th17 cell responses in the joint of RA individuals.

RA-like inflammatory profiles and function of CD1c$^+$ cDCs can be induced upon exposure to intracellular dsDNA

Our initial transcriptional study showed that innate pathways such as TLR and the inflammasome are altered in CD1c$^+$ cDC from RA patients and this is associated with increased surface expression of CD64. Previous studies showed the induction of CD64$^+$ cells in response to intracellular nucleic acids (39), which might also involve the activation of TLR or inflammasome components. Therefore, we asked whether the inflammatory cytokine profiles observed in CD1c$^+$ cDCs from RA individuals might be

associated with innate sensing of nucleic acids. To this end, we incubated healthy PB cDCs (mainly enriched in CD1c$^+$ cDCs; Supplemental Figure 7A) with nanoparticles loaded with dsDNA or Poly (I:C), to mimic intracellular exposure. CD1c$^+$ cDCs stimulated with nanoparticles containing dsDNA recapitulated cytokine/TLR signatures from this subset in RA patients inducing significantly higher levels of IL-1β, IL-8, CCL3, IL-23 and TNFα transcripts compared to those cells exposed to Poly (I:C), which expressed higher levels of IL-12 and IFNβ (Figure 5A; Supplemental Figure 7B). Functionally, primary CD1c$^+$ cDCs exposed to dsDNA induced increased proportions of total IL-17$^+$ CD4$^+$ T cells in vitro, and the majority of these cells were characterized by a pathogenic IL-17$^+$ IFNγ$^+$ phenotype (Figure 5B; Supplemental Figure 7C). Interestingly, induction of IL-17$^+$ CD4$^+$ T cells in the presence of dsDNA-stimulated cDCs was not due to proliferation of existing Th17 cells (Figure 5C, Supplemental Figure 7D) or differentiation from naïve T cells (Supplemental Figure 7E). Instead, memory CXCR3$^+$ CD4$^+$ T lymphocytes were enriched in cells capable of co-expressing IL-17 and IFNγ and most likely accounted for the increase of pathogenic Th17 responses in the presence of DNA-primed DCs (Supplemental Figure 7F). Together, the data indicate that activation of CD1c$^+$ cDCs in response to dsDNA induces phenotypical and functional properties that are similar to the inflammatory profiles present in PB and SF CD1c$^+$ cDCs from RA patients.

IgG-dsDNA complexes induce inflammasome activation in CD1c$^+$ cDCs and RA-like phenotypical characteristics

We next investigated the molecular mechanisms connecting inflammatory profiles on CD1c$^+$ cDCs from RA patients with intracellular sensing dsDNA, FcγR and specific pathways driving innate immune activation. Increased levels of CD64 are present on

circulating CD1c$^+$ cDCs in RA patients (Figure 1C; Supplemental Figure 2D), and expression of molecules associated with FcR-related-signaling (SYK, GBP1, PLC or PI3K) (40) were differentially affected on PB and SF CD1c$^+$ cDCs from RA subjects (Figure 6A, Supplemental Figure 4A). Therefore, our data suggest that FcR could contribute to the activation of CD1c$^+$ cDC from RA patients. We further analyzed additional PRR pathways that were previously predicted from our RNA-seq dataset (Figure 2B) and which might participate in the activation of CD1c$^+$ cDCs. The majority of DEG defining the TLR signature of circulating CD1c$^+$ cDCs from RA individuals included MAPK1, TLR5, MAP2K6, MAP2K4, CD40, TRAF6, TLR10, JUN, FOS (Supplemental Figure 4B, left). MAPK1 and MAP2K4 also tended to be increased in SF CD1c$^+$ cDC compared to the same population from the PB of HC individuals (Supplemental Figure 4B, right). Interestingly, some of these TLR-associated genes have also been involved in TLR2/4/5, TNFα and IL-1β mediated-inflammasome signaling (41-45), and created a unique interconnected signature in this subset from RA subjects (Supplemental Figure 4C). Furthermore, induction of IL-1β, IL-8 and CCL3 has been linked to inflammasome recognition of DNA-containing immunocomplexes, intracellular oxidized-DNA and to the expression of CD64 (46-50). Therefore, we assessed whether dsDNA associated with immunoglobulins could trigger the inflammatory cytokine signatures associated with the inflammasome in CD1c$^+$ cDCs. As shown in Figure 6B, CD1c$^+$ cDCs stimulated with dsDNA preincubated with human IgGs significantly induced higher mRNAs levels of IL-1β, IL-8 and CCL3 similarly to naked dsDNA. In contrast, IgG alone did not induce significant changes on cytokine expression (Figure 6B). In addition, TLR and inflammasome cytokine signature induced after exposure to dsDNA-IgG complexes and soluble dsDNA was accompanied by higher expression levels of CD40 and CD64 on CD1c$^+$ cDCs (Figure 6C; Supplemental Figure 8A).

Moreover, we observed that CD1c$^+$ cDCs also secreted higher levels of IL1-β (Figure 6D), suggesting that the activation of the inflammasome might be taking place in CD1c$^+$ cDC from RA patients in vivo. Supporting this possibility, CD1c$^+$ cDC infiltrated in the synovial membrane from RA patients expressed high levels of the inflammasome mediator Caspase 1 (51) (Figure 6E). Moreover, pharmacological inhibition of Caspase 1 and NFκB prevented the maturation of CD1c$^+$ cDC in the presence of the dsDNA-IgG complexes and the transcription of IL1-β (Figure 6F). Interestingly, pharmacological inhibition of Caspase1 and NFκB led to a complete abrogation of CD1c$^+$ cDC activation and IL1-β expression in response to dsDNA-IgG complexes, while drugs specific for the NLRP3 inflammasome, previously involved in Mo activation in RA (32), led to a partial and less significant effect, suggesting that additional non-redundant inflammasome sensors and NFκB might be involved in the process. Collectively, our results indicate that innate sensing of dsDNA-IgG complexes might be a potential mechanism inducing inflammatory signatures and inflammasome activation patterns observed in CD1c$^+$ cDCs in RA patients.

NLRC4 differentially contributes to FcγR-mediated sensing of dsDNA, induction of CD64 and RA inflammatory and functional profiles in CD1c$^+$ cDCs

Finally, we mined our RNA-seq dataset to investigate whether specific sensors might be preferentially driving inflammasome activation in CD1c$^+$ cDCs in RA patients. We first compared gene expression of 18 transcripts present on our dataset associated with inflammasome activity in Mo, CD1c$^+$ and CD141$^+$ cDC from RA patients, regardless our previous significance and log2FC cutoff (Figure 7A-B). Only 8 of these genes passed our original filter of which 6 transcripts (CASP1, CASP8, NLRC4, NAIP, NLRP3, IL1-β) were preferentially changed in CD1c$^+$ cDC or altered both in these cells and Mo (NLRP3,

CASP1, NAIP). Notably, circulating CD1c$^+$ cDCs displayed significant differential upregulation and downregulation of NLRC4 and NLRP3 inflammasome sensors, respectively (Figure 7A; Supplemental Figure 8B). In contrast, we did not observe any inflammasome related gene that passed our significance and Log2FC criteria in PB CD141$^+$ cDCs from RA patients although they showed less significant differential levels of alternative AIM2, PYCARD or NOD2 and NLRP1 inflammasome sensors, respectively (52, 53) (Figure 7B; Supplemental Figure 8B). Interestingly, NLRC4 and NLRP3 have been involved in innate sensing of bacterial products, nucleic acids and TLR activation (46-50) and created specific differential signaling networks in these cells (Figure 7C). Moreover, higher expression of NLRC4 and lower levels of NLRP3 was validated by qPCR on circulating CD1c$^+$ cDC from RA patients, and cells from the SF presented similar patterns (Figure 7D-E).

To test whether either NLRC4 or NLRP3 inflammasomes could indeed differentially contribute to the detection of dsDNA-IgG complexes, we performed siRNA-mediated knock down in primary CD1c$^+$ cDCs (Supplemental Figure 8C). NLRC4 knock down in CD1c$^+$ cDCs most significantly prevented increase of IL-1β and IL-8 mRNA levels compared to baseline in response to dsDNA-IgG complexes, while silencing of NLRP3 had a less significant effect (Figure 7F; Supplemental Figure 8D). Moreover, downregulation of NLRC4 and NLRP3 had opposite effects on CCL3 transcription by primary CD1c$^+$ cDCs (Figure 7F). In contrast, silencing of alternative inflammasome sensors such as AIM2 did significantly affect the induction of inflammatory cytokines in CD1c$^+$ cDCs (Figure 7E, Supplemental Figure 8D). Moreover, NLRC4 downregulation by siRNA specifically prevented upregulation of CD64 in response to IgG-dsDNA complexes (Figure 7G). Importantly, silencing of NLRC4 and NLRP3 also reduced the ability of cDC primed with IgG-dsDNA complexes to induce pathogenic IFNγ$^+$ IL-17$^+$

CD4$^+$ T cells in vitro, suggesting that activation of the inflammasome is required for such functional specialization (Figure 7H). Unexpectedly, CCR2 was downregulated in response to IgG-dsDNA complexes and this was also prevented by NLRC4 silencing (Supplemental Figure 8E). Therefore, preferential crosstalk between NLRC4 with FcγRs such as CD64, might drive inflammasome mediated inflammatory responses to intracellular dsDNA and IgG complexes in CD1c$^+$ cDCs from RA patients while interactions between this and other inflammasome sensors are required to acquire Th17-activating functional abilities.

DISCUSSION

The present translational study compared in parallel specific phenotypical, transcriptional and functional alterations of $CD1c^+$ and $CD141^+$ cDCs as well as Mo from PB and SF from RA patients, therefore providing novel cell subset-specific contribution to chronic inflammation and perpetuation of RA pathology. We have shown that $CD1c^+$ cDCs, like $CD141^+$ cDCs, are decreased in the blood of untreated RA patients and found in high frequencies in inflamed SF from treated patients, in agreement with other studies (22, 26). In addition, we have shown that treatment more significantly induces the recovery of circulating $CD1c^+$ cDC and this is associated with clinical improvement, supporting that these cells actively contribute to chronicity of RA pathology. In contrast, no significant changes in Mo subsets were observed between our control cohort and RA patients, which is not in agreement with previous studies reporting an increase in circulating transitional $CD16^+$ $CD14^{Hi}$ Mo. Such differences might be due to the age of our "early initiation" RA cohort, almost 10 years younger than those cohorts recruited in previous studies (54). This aspect is particularly relevant since higher levels of basal inflammation in older individuals have been associated to increased circulating $CD16^+$ Mo at baseline (55, 56), and might explain some of the results obtained with our cohort. Importantly, we identify expression of CD64 on $CD1c^+$ cDCs as a new marker also for this cell type, which to date had only been described for Mo for RA patients (36). The expression of this molecule is enriched in a migratory CCR2 subset of $CD1c^+$ cDCs, which are highly enriched in the SF of RA patients. Interestingly, CCR2 has been traditionally associated to recruitment of Mo in response to MCP-1 to inflamed sites (37) and has been recently associated with RA activity (38). We now provide evidence that $CD1c^+$ cDC might be using similar mechanisms to be recruited to inflamed synovial membrane. However, further studies addressing functionality of this chemokine receptor in cDCs are needed. In addition, our

RNA-seq analysis identifies specific transcriptional signatures for different myeloid subsets from RA patients.

Some of the limitations of our study include the difficulty of obtaining SF samples from untreated patients and healthy subjects, which might significantly affect levels of inflammation and reduce the resolution of our analysis. In addition, different controls used to compare expression levels in circulating and synovial cDCs might also affect our ability to detect differential expression of genes mediating inflammatory responses such as IL-1. On the other hand, due to sample availability, we could not study the impact of circulating and synovial DCs on pathogenic $CD4^+$ T cell responses dynamics on patients at the same stage of RA pathology, which could have limited our ability to stablish more direct associations. In this regard, the synovial membrane sections from patients with advanced disease used in our histology study might have limited our ability to detect higher frequencies of pathogenic Th1/Th17 cells in the tissue. Moreover, differences in gene expression patterns in myeloid cells from SF from RA patients compared to their circulating homologues or alternative inflammatory conditions such as CPPD-associated arthritis, might reflect either the selective migration of activated cells or different stages of activation in these two distinct immunopathogenic contexts. Therefore, future studies are needed to discriminate between these possibilities. Despite these limitations, we have identified specific transcriptional FcR, TLR and inflammasome signatures differentially altered in $CD1c^+$ cDC from both PB and SF. Interestingly, the ability of SF $CD1c^+$ cDCs to induce secretion of IL-17 by $CD4^+$ T cells has been previously reported (26), although it was not compared in parallel with Mo and $CD141^+$ cDCs.

In the present study, we describe for the first time that SF $CD1c^+$ cDCs from RA patients preferentially display a high capability to activate pathogenic $IL-17^+$ $IFNγ^+$ $CD4^+$ T cells involved in autoimmune diseases (8-10). This is particularly relevant, given the recent

evidence implication of these cells in RA pathology in patients (57) and in animal models (58). In fact, we demonstrate that CD141$^+$ cDCs do not efficiently support Th17 responses but future studies should address whether both cDC subsets functionally cooperate during disease pathogenesis. While recent data on the blockade of IL-17 did not yield as promising results in clinical trials as initially expected (59), it is important to highlight that Th1/Th17 cells have been shown to produce additional inflammatory cytokines such as GM-CSF (60), and it has been recently shown that the blockade of the receptor for this cytokine with mavrilimumab has an impact improving clinical parameters in RA patients (61). Moreover, we report enhanced abilities of dsDNA-stimulated CD1c$^+$ cDC differentiation of CXCR3$^+$ CD4$^+$ T cells into pathogenic Th1/Th17 T cells, supporting their capacity to increase memory T cells plasticity in RA patients (62). Moreover, we provide evidence that dsDNA-IgG complexes might act as DAMPs and trigger pathogenic activation of CD1c$^+$ cDC in a Caspase 1/NKκB-dependent manner. This possibility is supported by previous studies reporting extracellular dsDNA from neutrophils through NETosis in RA patients (63). In addition to CD4$^+$ T cells, our data suggest that CD1c$^+$ cDC and Mo might be able to induce activation of cytotoxic CD107a$^+$ IFNγ$^+$ CD8$^+$ T cells. It has been recently described that activated granzyme K$^+$ CD8$^+$ T cells in the inflamed synovium might contribute to RA pathology (64). However, further studies are required to determine whether CD8$^+$ T cells activated in the presence of CD1c$^+$ cDC can specifically acquire the phenotypical and functional properties of this particular granzyme K$^+$ CD8$^+$ T cell subset. Therefore, we provide a novel functional mechanism whereby CD1c$^+$ cDCs might contribute to the perpetuation of chronic inflammation and RA pathology.

At the molecular level, we have identified NLRC4 as a novel inflammasome sensor differentially upregulated in CD1c$^+$ cDCs from RA patients which seems to be non-

redundantly involved in the detection of intracellular dsDNA. In contrast, downregulated expression of NLRP3 in CD1c$^+$ cDCs from RA patients suggests a limited role of this sensor driving activation of this particular subset, in agreement with the presented siRNA-knock down results. However, NLRP3 can recognize a variety of DAMPs including nucleic acids (48-50) and can mediate activation of Mo after FcγR stimulation with IgG and antigen immunocomplexes (39, 65, 66), which supports a relevant role of this sensor in other myeloid subsets such as Mo. On the other hand, NLRC4 inflammasome can be activated in response to bacterial components (67, 68) and innate antiviral responses (69, 70). Importantly, the expression of NLRC4 is also associated with autoimmune disorders in the nervous system (71, 72) or the skin (73). Interestingly, there was no information on the role of this molecule on dsDNA sensing or association with Fc receptors in specific innate immune cell subsets or in the context of RA. Remarkably, the expression of NLRC4 and NLRP3 seems to stablish a balance that tightly regulates CCL3 in CD1c$^+$ cDCs in response to dsDNA in a subset-specific manner. Therefore, these two molecules might represent two non-redundant therapeutic targets for RA. Supporting this interpretation, mutation on NLRC4 might affect predisposition to develop inflammatory diseases such as RA (74). While recent studies in animal models suggest that NLRP3 inhibitors might be useful for treating RA (33), our data suggest that combined targeting of CD64 and both NLRC4 and NLRP3 inflammasomes might be a useful synergistic strategy to reduce aberrant inflammatory responses in CD1c$^+$ cDC as well as other myeloid subset and prevent RA progression. A standing question is whether NLRC4 and NLRP3 might act in conjunction or independently to TLR stimulation. Our data are consistent with high levels of TLR activation on CD1c$^+$ cDCs. However, the implication of TLRs involved, components of the signaling cascade and the interaction with the inflammasome has not been addressed in our study. Thus, more studies are required to

fully understand these aspects and the novel nucleic-acid sensing pathways and their potential as therapeutic targets in human CD1c$^+$ cDCs and Mo. Together, our study provides novel relevant information about the contribution of CD1c$^+$ cDCs to cellular networks participating in RA pathogenesis and identifies crosstalk between the NLRC4 inflammasome and CD64 as potential future therapeutic targets for CD1c$^+$ cDCs in RA patients.

MATERIALS AND METHODS

Study Participants

Peripheral blood mononuclear cells (PBMC) were obtained from patients included in PEARL (Princesa Early Arthritis Register Longitudinal) study. Twenty-five untreated individuals (15 fulfilling RA criteria and 10 undifferentiated arthritis [UA]), were studied. Their baseline features are shown in Supplemental Table 1. For comparison purposes, PBMC from 17 healthy controls (HC) were isolated from Buffy coat samples obtained from the Centro de Transfusiones Comunidad de Madrid and from 13 age and sex matched individuals recruited from Hospital de la Princesa sample repository (Supplemental Table 1). Longitudinal studies with additional RA patients were performed after 1 and 2 years in treatment (Supplemental Table 3). Mononuclear cells obtained from SF samples drained for therapeutic or diagnostic procedures from 16 individuals presenting different rheumatic disorders including RA, Calcium Pyrophosphate Deposition (CPPD) crystals-associated arthropathy and Spondyloarthritis receiving different treatment regimens (see Supplemental Table 2) were used for additional phenotypical and transcriptional validation studies.

Flow cytometry phenotypical analysis and cell sorting

Ex vivo and cultured PBMC were stained with APC-H7 (Tonbo Biosciences) or Brilliant Violet 405 (Molecular Probes) viability dye in the presence of different panels of monoclonal antibodies against lineage (Lin; CD3, CD19, CD20, CD56), CD14, CD16, CD40, CD86, ILT4, HLA-DR, CD11c, CD1c, CD141, CD64 and PDL1 (Biolegend). Samples were analyzed on a Fortessa cytometer (BD Biosciences) at Centro Nacional de Investigaciones Cardiovasculares (CNIC, Madrid, Spain). Analysis of individual and multiparametric flow cytometry data was performed using FlowJo software (Tree Star).

For the transcriptional studies, viable human Lin^{-} CD14^{-} CD11c^{+} HLADR^{+} CD1c^{+} cDCs, CD14^{-} CD11c^{+} HLADR^{+} CD141^{+} cDCs and total CD14^{+} monocytes were sorted using a FACS Aria II sorter (BD Biosciences) from either PBMC from n=4 untreated RA patients and n=4 healthy controls (HC) or synovial fluid from n=3 individuals with RA and n=3 suffering mechanic CPPD crystals-associated arthritis.

Gene expression analysis by RNA-Seq and Computational data analysis

RNA was isolated from sorted Mo, CD1c^{+} and CD141^{+} cDC populations from PB from n=4 untreated RA patients and n=4 HC, or from the SF of n=3 RA and n=3 CPPD crystals-associated arthritis patients using the RNeasy Micro Kit (Qiagen). Quality and integrity of each RNA sample was checked using a Bioanalyzer 2100 instrument (Agilent) before proceeding to RNA-seq protocol. Subsequently, selected RNAs from cDCs were used to amplify the cDNA using the SMART-Seq v4 Ultra Low Input RNA Kit (Clontech-Takara). 1 ng of amplified cDNA was used to generate barcoded libraries using the Nextera XT DNA library preparation kit (Illumina). The size of the libraries was checked using the Agilent 2100 Bioanalyzer High Sensitivity DNA chip and their concentration was determined using the Qubit® fluorometer (ThermoFisher Scientific). RNA from circulating Mo was processed as follows. 200 ng of total RNA were used to generate barcoded RNA-seq libraries using the NEBNext Ultra II Directional RNA Library Prep Kit (New England Biolabs Inc). Libraries were sequenced on a HiSeq 2500 (Illumina) and on a HiSeq 4000 and processed with RTA v1.18.66.3. FastQ files for each sample were obtained using bcl2fastq v2.20.0.422 software (Illumina).

Sequencing reads were aligned to the human reference transcriptome (GRCh38 v91) and quantified with RSem v1.3.1 (75). Raw counts were normalized with TPM (Transcripts per Million) and TMM (Trimmed Mean of M-values) methods, transformed into log2

expression (log2(rawCount+1)) and compared to calculate fold-change and corrected p-value. Only those genes expressed with at least 1 count in a number of samples equal to the number of replicate samples of the condition with less replicates were taken into account. Gene expression changes were considered significant if associated to Benjamini and Hochberg adjusted p-value <0.05 and a log2 fold change in gene expression greater than 1.5 and lower than -1.5.

Heatmaps were generated with Morpheus online tool from Broad Institute (https://software.broadinstitute.org/morpheus). Finally, pathway analysis and visualization of gene networks for each differentially expressed genes (DEG) list was performed using Ingenuity Pathway Analysis (Qiagen), DAVID Bioinformatics Resources 6.8, Metascape (http://metascape.org/gp/index.html#/main/step1) and NetworkAnalyst (76) Softwares.

Data availability

RNA-seq data from the study has been deposited on the public Gene Expression Omnibus (GEO) repository, accession number: GSE157047 (https://www.ncbi.nlm.nih.gov/geo/query/acc.cgi?acc=GSE157047)

Validation of gene expression by RT-qPCR

RNA was isolated from sorted PB or SF myeloid subsets using RNeasy Micro Kit (Qiagen) according to manufacturer´s instructions. cDNA was synthesized using the reverse transcription kit (Promega) and gene expression was analyzed by semiquantitative PCR using the SYBR Green assay GoTaq® qPCR Master Mix (Promega) with standardized primers (Metabion) on a StepOne Real-Time PCR system (Applied Biosystems). Relative gene expression was normalized to β-actin detection.

siRNA-mediated gene knockdown

Gene knockdown of NLRP3, NLRC4 and AIM2 was performed by nucleofection of fresh primary cDCs (Amaxa4D-Nucleofector, Lonza) with specific siRNAs (SMART-pool, Horizon Discovery) or irrelevant scramble siRNA according to manufacturer´s instructions. siRNA-mediated knockdown was analyzed after 24h by RT-qPCR.

Isolation of primary DCs and T cells

Total cDCs enriched for CD1c$^+$ cDCs were purified from total PBMC suspensions by immunomagnetic enrichment (purity >90%) using the Human Myeloid DC Enrichment Kit (STEMCELL). Total T cells and CD4$^+$ T cells were isolated using the Untouched Human T cell and CD4$^+$ T cell kits (Invitrogen), leading to a cell suspension of purity >95%. For some experiments, circulating naïve and CXCR3$^+$ memory CD4$^+$ T cells were isolated from previously purified total CD4$^+$ lymphocyte fractions using a manual EasySep Human Naïve CD4$^+$ T Cell Isolation Kit (STEMCELL) or using PE-labelled anti-CXCR3 mAb (Biolegend) plus anti-PE microbeads (Miltenyi Biotec) and the AutoMACS cell sorter (Miltenyi Biotec), respectively. For functional assays with cells present in the SF, total CD14$^+$ Mo, CD1c$^+$ and CD141$^+$ cDCs were sorted by flow cytometry in parallel as previously described.

In vitro stimulation of DCs and functional assays

Primary cDCs were cultured for 24h in the presence of polymeric nano-particles (TransIT-X2, Mirus Bio) alone or pre-loaded with either 5µg of Salmon sperm dsDNA (Invitrogen), 5µg Poly I:C (SIGMA) according to manufacturer´s instructions. In other set of experiments, primary cDC were incubated with human IgG alone (SIGMA) or in

complexes with the mentioned Salmon sperm dsDNA. Expression of CD86 and CD40 was analyzed by flow cytometry. In some experiments, levels of CD64 and CCR2 were also assessed. Subsequently, DCs were co-cultured with allogeneic total, naïve or CXCR3$^+$ CD4$^+$ T cells for 5 days at a 1:1 ratio in media supplemented with 25 IU/ml IL-2 (Peprotech). In some experiments, cDCs were previously nucleofected with siRNAs targeting candidate intracellular sensors (see above). Intracellular expression of IFNγ and IL-17 on cultured T cells was analyzed by flow cytometry at the end of the assay at day 5 after restimulation with 0.25 μg/mL PMA (SIGMA) and Ionomycin (SIGMA) for 1h and cultured for 4h in the presence of 0.5 μg/mL brefeldin A (SIGMA) and 0.005 mM monensin. In some experiments, T cells were pre-labelled with Violet CellTrace proliferation tracker (Invitrogen). In some experiments, cDCs or MDDCs were stimulated with 5 μg of Salmon dsDNA and preincubated for 3h at 37°C in the presence of media or 100μg/ml human IgG to facilitate complex formation. After 24h, cytokine expression was analyzed by RT-qPCR.

Histological analysis of synovial tissue

Synovial membrane sections were paraffin-embedded and segmented in fragments of 3-5 μm of thickness in a Leica microtome. Tissue sections deparaffinization, hydration and target retrival were performed with a PT-LINK (Dako) previous to staining. For staining of CD1c$^+$ cDCs we used a mouse anti-human CD1c and rabbit anti-human HLA-DR primary antibodies (Abcam). Expression of IL-17 or Caspase 1 was analyzed with either a goat anti-IL-17 or a goat anti-Caspase 1 primary antibodies (R&D) and expression of IFNγ was evaluated using a rabbit anti-IFNγ antibody (Abcam). Secondary antibodies used included a donkey anti-rabbit Alexa Fluor 488, donkey anti-mouse Alexa Fluor 647 and donkey anti-goat Alexa Fluor 568 (ThermoFisher Scientific) as secondary antibodies.

Images were taken with a Leica TCS SP5 confocal and processed with the LAS AF software. Images were further processed using the Image J software.

Statistics

Gene expression changes were considered significant following the criteria described in section Gene expression analysis by RNA-Seq and Computational data analysis from section. Significance of differences between the cells from different or within the same patient cohorts were assessed using Mann Whitney U or Wilcoxon matched-pairs signed-rank tests. Multiple comparison correction using a Kruskal-Wallis test with post-hoc Dunn's test, the Bonferroni correction or False Discovery Rate (FDR) methods was applied when appropriate. P value lower than 0.05 were considered significant.

Study approval

All subjects gave written informed consent and the study was approved by the Institutional Review Board of Hospital Universitario de La Princesa (Register Number 3515) and following the Helsinki declaration.

AUTHOR CONTRIBUTIONS

E.M.G., I.G.A, F.S.M., S.C., C.D.A, M.C.M and A.T.M developed the research idea and study concept, designed the study and wrote the manuscript;

E.M.G. and I.G.A. supervised the study;

C.D.A., M.C.M and A.T.M designed and conducted most experiments and equally contributed to the study;

O.P. and I.T. participated in the functional analysis of si-RNA-treated DC;

I.G.A, S.C. and F.S.M. provided peripheral blood and synovial fluid samples from study patient cohorts;

A.T.M. S.C. and I.G.A. provided information of clinical parameters during the study;

E.V.L provided bioinformatic support for computational RNA-Seq data analyses and supervised statistical analysis;

A.A.F, R.M.V, A.D. performed and collaborated in the RNA-seq experiments;

E.M.G and M.C.M. performed pathway analysis of transcriptional data;

C.D.A, M.C.M. and I.S.C. performed phenotypical analysis and sorting of samples;

D.C.F. participated in flow cytometry analysis;

A.R. and V.D.Y provided access and support for sample cell sorting;

R.L. and G.H.B. provided RA synovial membrane specimens for histological analyses;

H.D.F. and F.S.M. provided qPCR reagents and cell samples from healthy donors and participated in data discussion.

ACKNOWLEDGEMENTS

REFERENCES

1.   Sebbag M, Chapuy-Regaud S, Auger I, Petit-Texeira E, Clavel C, Nogueira L, et al. Clinical and pathophysiological significance of the autoimmune response to citrullinated proteins in rheumatoid arthritis. Joint Bone Spine. 2004;71(6):493-502.

2.   Chapuy-Regaud S, Nogueira L, Clavel C, Sebbag M, Vincent C, Serre G. IgG subclass distribution of the rheumatoid arthritis-specific autoantibodies to citrullinated fibrin. Clinical and experimental immunology. 2005;139(3):542-50.

3.   Szodoray P, Szabo Z, Kapitany A, Gyetvai A, Lakos G, Szanto S, et al. Anti-citrullinated protein/peptide autoantibodies in association with genetic and environmental factors as indicators of disease outcome in rheumatoid arthritis. Autoimmun Rev. 2010;9(3):140-3.

4.   Shen H, Goodall JC, Hill Gaston JS. Frequency and phenotype of peripheral blood Th17 cells in ankylosing spondylitis and rheumatoid arthritis. Arthritis and rheumatism. 2009;60(6):1647-56.

5.   Alvandpur N, Tabatabaei R, Tahamoli-Roudsari A, Basiri Z, Behzad M, Rezaeepoor M, et al. Circulating IFN-gamma producing CD4+ T cells and IL-17A producing CD4+ T cells, HLA-shared epitope and ACPA may characterize the clinical response to therapy in rheumatoid arthritis patients. Human immunology. 2020.

6.   Li SG, Quayle AJ, Shen Y, Kjeldsen-Kragh J, Oftung F, Gupta RS, et al. Mycobacteria and human heat shock protein-specific cytotoxic T lymphocytes in rheumatoid synovial inflammation. Arthritis and rheumatism. 1992;35(3):270-81.

7.   Nistala K, Adams S, Cambrook H, Ursu S, Olivito B, de Jager W, et al. Th17 plasticity in human autoimmune arthritis is driven by the inflammatory environment. Proceedings of the National Academy of Sciences of the United States of America. 2010;107(33):14751-6.

8.   Tsanaktsi A, Solomou EE, Liossis SC. Th1/17 cells, a subset of Th17 cells, are expanded in patients with active systemic lupus erythematosus. Clin Immunol. 2018;195:101-6.

9.   Kebir H, Ifergan I, Alvarez JI, Bernard M, Poirier J, Arbour N, et al. Preferential recruitment of interferon-gamma-expressing TH17 cells in multiple sclerosis. Ann Neurol. 2009;66(3):390-402.

10.   Ahn Y, Hwang JH, Zheng Z, Bang D, Kim DY. Enhancement of Th1/Th17 inflammation by TRIM21 in Behcet's disease. Scientific reports. 2017;7(1):3018.

11.   O'Keeffe M, Mok WH, Radford KJ. Human dendritic cell subsets and function in health and disease. Cellular and molecular life sciences : CMLS. 2015.

12.   Jongbloed SL, Kassianos AJ, McDonald KJ, Clark GJ, Ju X, Angel CE, et al. Human CD141+ (BDCA-3)+ dendritic cells (DCs) represent a unique myeloid DC subset that cross-presents necrotic cell antigens. The Journal of experimental medicine. 2010;207(6):1247-60.

13.   Yang J, Zhang L, Yu C, Yang XF, Wang H. Monocyte and macrophage differentiation: circulation inflammatory monocyte as biomarker for inflammatory diseases. Biomark Res. 2014;2(1):1.

14.   Rana AK, Li Y, Dang Q, Yang F. Monocytes in rheumatoid arthritis: Circulating precursors of macrophages and osteoclasts and, their heterogeneity and plasticity role in RA pathogenesis. Int Immunopharmacol. 2018;65:348-59.

15. Soler Palacios B, Estrada-Capetillo L, Izquierdo E, Criado G, Nieto C, Municio C, et al. Macrophages from the synovium of active rheumatoid arthritis exhibit an activin A-dependent pro-inflammatory profile. The Journal of pathology. 2015;235(3):515-26.

16. Fang Q, Zhou C, Nandakumar KS. Molecular and Cellular Pathways Contributing to Joint Damage in Rheumatoid Arthritis. Mediators Inflamm. 2020;2020:3830212.

17. Takakubo Y, Takagi M, Maeda K, Tamaki Y, Sasaki A, Asano T, et al. Distribution of myeloid dendritic cells and plasmacytoid dendritic cells in the synovial tissues of rheumatoid arthritis. The Journal of rheumatology. 2008;35(10):1919-31.

18. Solano-Galvez SG, Tovar-Torres SM, Tron-Gomez MS, Weiser-Smeke AE, Alvarez-Hernandez DA, Franyuti-Kelly GA, et al. Human Dendritic Cells: Ontogeny and Their Subsets in Health and Disease. Med Sci (Basel). 2018;6(4).

19. Rhodes JW, Tong O, Harman AN, Turville SG. Human Dendritic Cell Subsets, Ontogeny, and Impact on HIV Infection. Frontiers in immunology. 2019;10:1088.

20. Gilliet M, Cao W, Liu YJ. Plasmacytoid dendritic cells: sensing nucleic acids in viral infection and autoimmune diseases. Nature reviews Immunology. 2008;8(8):594-606.

21. Jongbloed SL, Benson RA, Nickdel MB, Garside P, McInnes IB, Brewer JM. Plasmacytoid dendritic cells regulate breach of self-tolerance in autoimmune arthritis. Journal of immunology. 2009;182(2):963-8.

22. Cooles FAH, Anderson AE, Skelton A, Pratt AG, Kurowska-Stolarska MS, McInnes I, et al. Phenotypic and Transcriptomic Analysis of Peripheral Blood Plasmacytoid and Conventional Dendritic Cells in Early Drug Naive Rheumatoid Arthritis. Frontiers in immunology. 2018;9:755.

23. Anderson DA, 3rd, Murphy KM, Briseno CG. Development, Diversity, and Function of Dendritic Cells in Mouse and Human. Cold Spring Harbor perspectives in biology. 2017.

24. Villani AC, Satija R, Reynolds G, Sarkizova S, Shekhar K, Fletcher J, et al. Single-cell RNA-seq reveals new types of human blood dendritic cells, monocytes, and progenitors. Science. 2017;356(6335).

25. Canavan M, Walsh AM, Bhargava V, Wade SM, McGarry T, Marzaioli V, et al. Enriched Cd141+ DCs in the joint are transcriptionally distinct, activated, and contribute to joint pathogenesis. JCI Insight. 2018;3(23).

26. Moret FM, Hack CE, van der Wurff-Jacobs KM, de Jager W, Radstake TR, Lafeber FP, et al. Intra-articular CD1c-expressing myeloid dendritic cells from rheumatoid arthritis patients express a unique set of T cell-attracting chemokines and spontaneously induce Th1, Th17 and Th2 cell activity. Arthritis research & therapy. 2013;15(5):R155.

27. Diogo D, Okada Y, Plenge RM. Genome-wide association studies to advance our understanding of critical cell types and pathways in rheumatoid arthritis: recent findings and challenges. Curr Opin Rheumatol. 2014;26(1):85-92.

28. Suzuki A, Yamamoto K. From genetics to functional insights into rheumatoid arthritis. Clin Exp Rheumatol. 2015;33(4 Suppl 92):S40-3.

29. Torices S, Alvarez-Rodriguez L, Varela I, Munoz P, Balsa A, Lopez-Hoyos M, et al. Evaluation of Toll-like-receptor gene family variants as prognostic biomarkers in rheumatoid arthritis. Immunology letters. 2017;187:35-40.

30. Okada Y, Eyre S, Suzuki A, Kochi Y, Yamamoto K. Genetics of rheumatoid arthritis: 2018 status. Annals of the rheumatic diseases. 2019;78(4):446-53.

31. Roers A, Hiller B, Hornung V. Recognition of Endogenous Nucleic Acids by the Innate Immune System. Immunity. 2016;44(4):739-54.
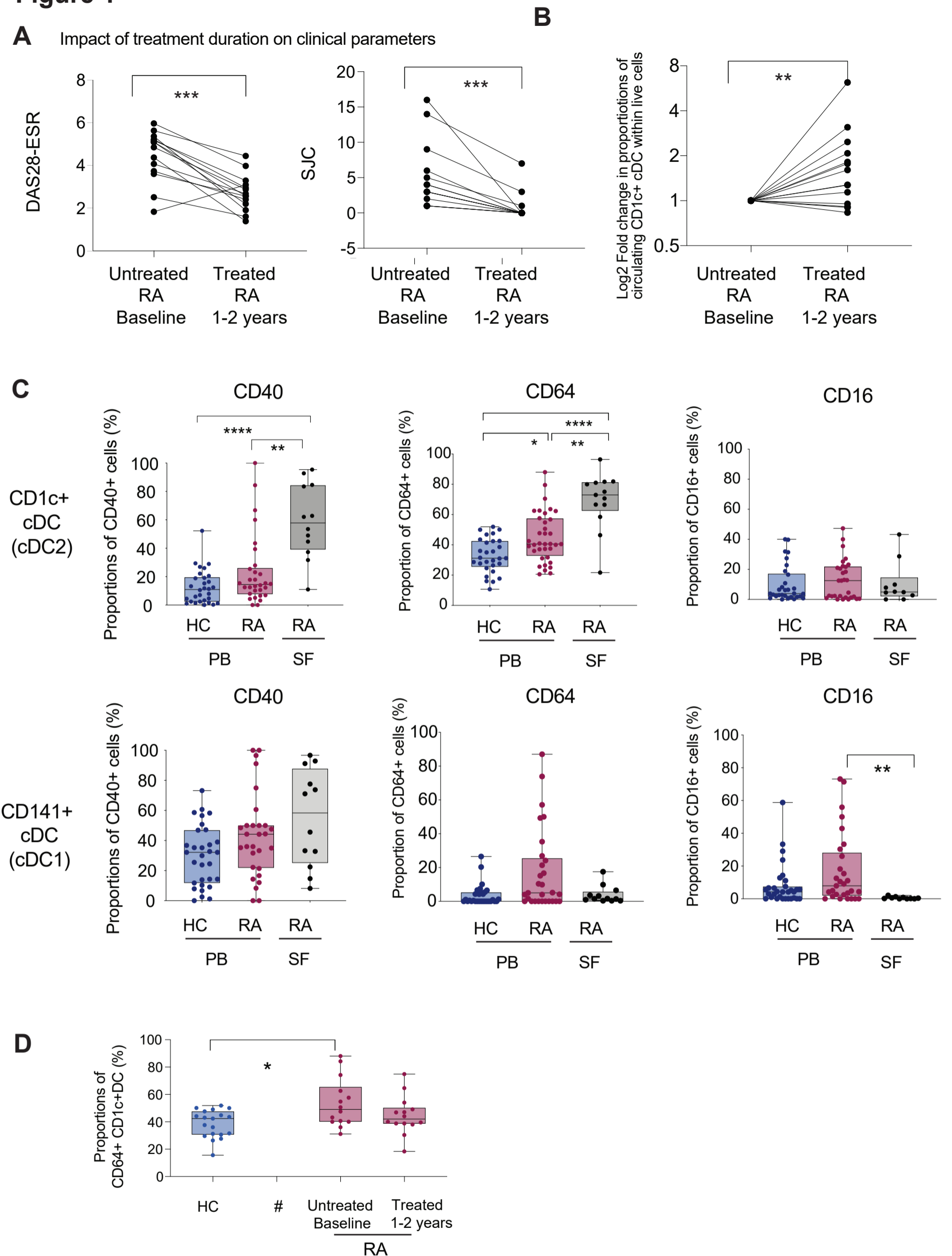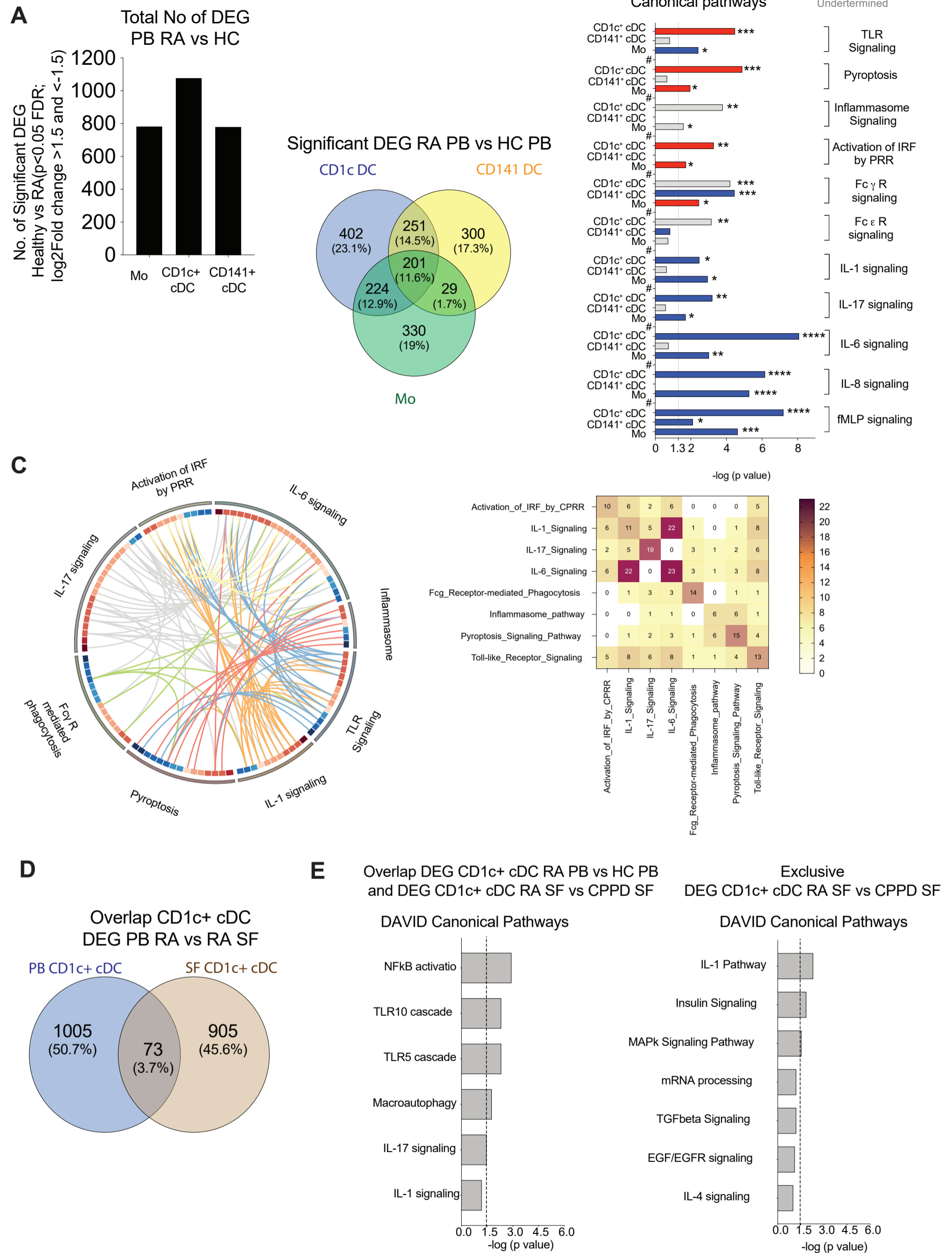
32.   Jäger E, Murthy S, Schmidt C, Hahn M, Strobel S, Peters A, et al. Calcium-sensing receptor-mediated NLRP3 inflammasome response to calciprotein particles drives inflammation in rheumatoid arthritis. Nature communications. 2020;11(1):4243.

33.   Guo C, Fu R, Wang S, Huang Y, Li X, Zhou M, et al. NLRP3 inflammasome activation contributes to the pathogenesis of rheumatoid arthritis. Clinical and experimental immunology. 2018;194(2):231-43.

34.   Michaud TL, Rho YH, Shamliyan T, Kuntz KM, Choi HK. The comparative safety of tumor necrosis factor inhibitors in rheumatoid arthritis: a meta-analysis update of 44 trials. Am J Med. 2014;127(12):1208-32.

35.   Gigliucci G, Massafra U, Frediani B, De Cata A, Gallelli L, Integlia D, et al. A review of network meta-analysis comparing biologics in the treatment of rheumatoid arthritis. Eur Rev Med Pharmacol Sci. 2020;24(4):1624-44.

36.   Luo Q, Xiao P, Li X, Deng Z, Qing C, Su R, et al. Overexpression of CD64 on CD14(++)CD16(-) and CD14(++)CD16(+) monocytes of rheumatoid arthritis patients correlates with disease activity. Exp Ther Med. 2018;16(3):2703-11.

37.   Zhu S, Liu M, Bennett S, Wang Z, Pfleger KDG, Xu J. The molecular structure and role of CCL2 (MCP-1) and C-C chemokine receptor CCR2 in skeletal biology and diseases. Journal of cellular physiology. 2021;236(10):7211-22.

38.   Moadab F, Khorramdelazad H, Abbasifard M. Role of CCL2/CCR2 axis in the immunopathogenesis of rheumatoid arthritis: Latest evidence and therapeutic approaches. Life Sci. 2021;269:119034.

39.   Martin-Gayo E, Cole MB, Kolb KE, Ouyang Z, Cronin J, Kazer SW, et al. A Reproducibility-Based Computational Framework Identifies an Inducible, Enhanced Antiviral State in Dendritic Cells from HIV-1 Elite Controllers. Genome biology. 2018;19(1):10.

40.   Futosi K, Fodor S, Mocsai A. Neutrophil cell surface receptors and their intracellular signal transduction pathways. Int Immunopharmacol. 2013;17(3):638-50.

41.   Walsh MC, Lee J, Choi Y. Tumor necrosis factor receptor- associated factor 6 (TRAF6) regulation of development, function, and homeostasis of the immune system. Immunological reviews. 2015;266(1):72-92.

42.   Brown J, Wang H, Hajishengallis GN, Martin M. TLR-signaling networks: an integration of adaptor molecules, kinases, and cross-talk. Journal of dental research. 2011;90(4):417-27.

43.   Grishman EK, White PC, Savani RC. Toll-like receptors, the NLRP3 inflammasome, and interleukin-1beta in the development and progression of type 1 diabetes. Pediatric research. 2012;71(6):626-32.

44.   López-Yglesias AH, Zhao X, Quarles EK, Lai MA, VandenBos T, Strong RK, et al. Flagellin induces antibody responses through a TLR5- and inflammasome-independent pathway. Journal of immunology. 2014;192(4):1587-96.

45.   Zhang B, Chassaing B, Shi Z, Uchiyama R, Zhang Z, Denning TL, et al. Viral infection. Prevention and cure of rotavirus infection via TLR5/NLRC4-mediated production of IL-22 and IL-18. Science. 2014;346(6211):861-5.

46.   Ha H, Debnath B, Neamati N. Role of the CXCL8-CXCR1/2 Axis in Cancer and Inflammatory Diseases. Theranostics. 2017;7(6):1543-88.

47.   Dib B, Lin H, Maidana DE, Tian B, Miller JB, Bouzika P, et al. Mitochondrial DNA has a pro-inflammatory role in AMD. Biochim Biophys Acta. 2015;1853(11 Pt A):2897-906.
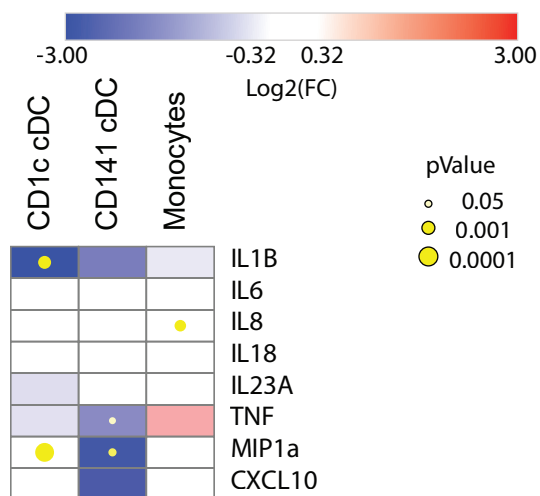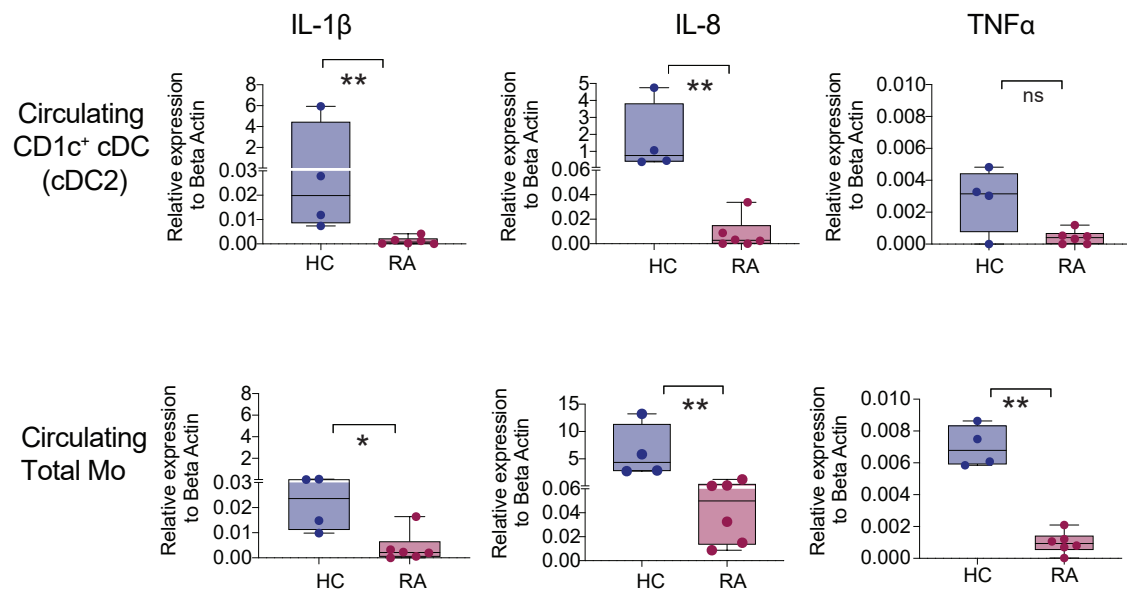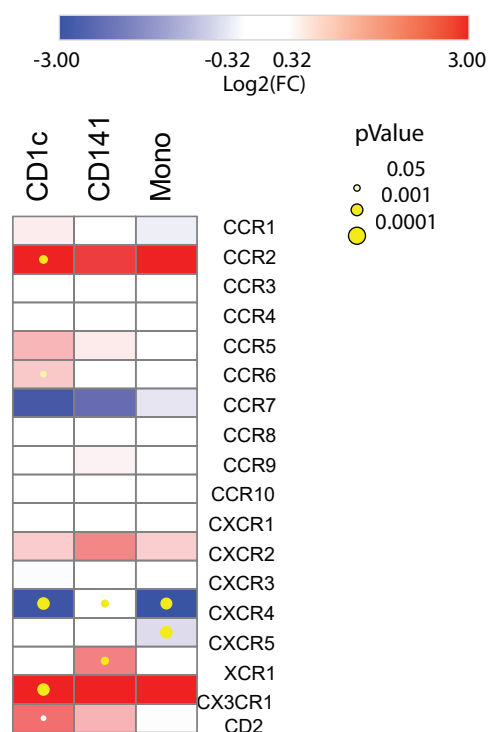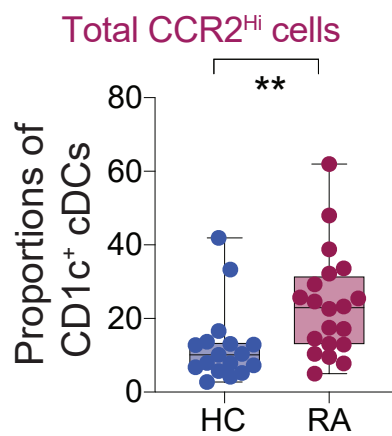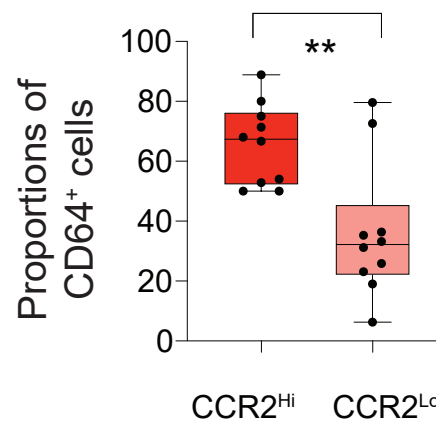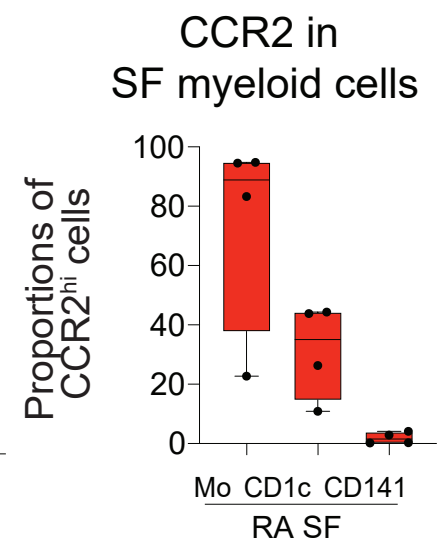
48.   Allen IC, Scull MA, Moore CB, Holl EK, McElvania-TeKippe E, Taxman DJ, et al. The NLRP3 inflammasome mediates in vivo innate immunity to influenza A virus through recognition of viral RNA. Immunity. 2009;30(4):556-65.

49.   Shimada K, Crother TR, Karlin J, Dagvadorj J, Chiba N, Chen S, et al. Oxidized mitochondrial DNA activates the NLRP3 inflammasome during apoptosis. Immunity. 2012;36(3):401-14.

50.   Kailasan Vanaja S, Rathinam VA, Atianand MK, Kalantari P, Skehan B, Fitzgerald KA, et al. Bacterial RNA:DNA hybrids are activators of the NLRP3 inflammasome. Proceedings of the National Academy of Sciences of the United States of America. 2014;111(21):7765-70.

51.   Hayward JA, Mathur A, Ngo C, Man SM. Cytosolic Recognition of Microbes and Pathogens: Inflammasomes in Action. Microbiology and molecular biology reviews : MMBR. 2018;82(4).

52.   Jonsson KL, Laustsen A, Krapp C, Skipper KA, Thavachelvam K, Hotter D, et al. IFI16 is required for DNA sensing in human macrophages by promoting production and function of cGAMP. Nature communications. 2017;8:14391.

53.   Man SM, Karki R, Kanneganti TD. AIM2 inflammasome in infection, cancer, and autoimmunity: Role in DNA sensing, inflammation, and innate immunity. European journal of immunology. 2016;46(2):269-80.

54.   Tsukamoto M, Seta N, Yoshimoto K, Suzuki K, Yamaoka K, Takeuchi T. CD14(bright)CD16+ intermediate monocytes are induced by interleukin-10 and positively correlate with disease activity in rheumatoid arthritis. Arthritis research & therapy. 2017;19(1):28.

55.   Prajzlerová K, Kryštůfková O, Komarc M, Mann H, Hulejová H, Petrovská N, et al. The dysregulation of monocyte subpopulations in individuals at risk of developing rheumatoid arthritis. Rheumatology (Oxford). 2021;60(4):1823-31.

56.   Zhang L, Yao Y, Tian J, Jiang W, Zhou S, Chen J, et al. Alterations and abnormal expression of A20 in peripheral monocyte subtypes in patients with rheumatoid arthritis. Clinical rheumatology. 2021;40(1):341-8.

57.   Bazzazi H, Aghaei M, Memarian A, Asgarian-Omran H, Behnampour N, Yazdani Y. Th1-Th17 Ratio as a New Insight in Rheumatoid Arthritis Disease. Iranian journal of allergy, asthma, and immunology. 2018;17(1):68-77.

58.   Boldizsar F, Tarjanyi O, Nemeth P, Mikecz K, Glant TT. Th1/Th17 polarization and acquisition of an arthritogenic phenotype in arthritis-susceptible BALB/c, but not in MHC-matched, arthritis-resistant DBA/2 mice. International immunology. 2009;21(5):511-22.

59.   Taams LS. Interleukin-17 in rheumatoid arthritis: Trials and tribulations. The Journal of experimental medicine. 2020;217(3).

60.   Wade SM, Canavan M, McGarry T, Low C, Wade SC, Mullan RH, et al. Association of synovial tissue polyfunctional T-cells with DAPSA in psoriatic arthritis. Annals of the rheumatic diseases. 2019;78(3):350-4.

61.   Weinblatt ME, McInnes IB, Kremer JM, Miranda P, Vencovsky J, Guo X, et al. A Randomized Phase IIb Study of Mavrilimumab and Golimumab in Rheumatoid Arthritis. Arthritis Rheumatol. 2018;70(1):49-59.

62.   Leipe J, Pirronello F, Schulze-Koops H, Skapenko A. Altered T cell plasticity favours Th17 cells in early arthritis. Rheumatology (Oxford). 2020.

63.   Corsiero E, Pratesi F, Prediletto E, Bombardieri M, Migliorini P. NETosis as Source of Autoantigens in Rheumatoid Arthritis. Frontiers in immunology. 2016;7:485.

64.   Jonsson AH, Zhang F, Dunlap G, Gomez-Rivas E, Watts GFM, Faust HJ, et al. Granzyme K(+) CD8 T cells form a core population in inflamed human tissue. Science translational medicine. 2022;14(649):eabo0686.

65.   Castro-Dopico T, Dennison TW, Ferdinand JR, Mathews RJ, Fleming A, Clift D, et al. Anti-commensal IgG Drives Intestinal Inflammation and Type 17 Immunity in Ulcerative Colitis. Immunity. 2019;50(4):1099-114 e10.

66.   Zhang H, Li L, Liu L. FcgammaRI (CD64) contributes to the severity of immune inflammation through regulating NF-kappaB/NLRP3 inflammasome pathway. Life Sci. 2018;207:296-303.

67.   Halff EF, Diebolder CA, Versteeg M, Schouten A, Brondijk TH, Huizinga EG. Formation and structure of a NAIP5-NLRC4 inflammasome induced by direct interactions with conserved N- and C-terminal regions of flagellin. The Journal of biological chemistry. 2012;287(46):38460-72.

68.   Wu J, Fernandes-Alnemri T, Alnemri ES. Involvement of the AIM2, NLRC4, and NLRP3 inflammasomes in caspase-1 activation by Listeria monocytogenes. J Clin Immunol. 2010;30(5):693-702.

69.   Ravimohan S, Maenetje P, Auld SC, Ncube I, Mlotshwa M, Chase W, et al. A Common NLRC4 Gene Variant Associates With Inflammation and Pulmonary Function in Human Immunodeficiency Virus and Tuberculosis. Clin Infect Dis. 2019.

70.   Hornick EE, Dagvadorj J, Zacharias ZR, Miller AM, Langlois RA, Chen P, et al. Dendritic cell NLRC4 regulates influenza A virus-specific CD4 T cell responses through FasL expression. The Journal of clinical investigation. 2019;129(7):2888-97.

71.   Freeman L, Guo H, David CN, Brickey WJ, Jha S, Ting JP. NLR members NLRC4 and NLRP3 mediate sterile inflammasome activation in microglia and astrocytes. The Journal of experimental medicine. 2017;214(5):1351-70.

72.   Soares JL, Oliveira EM, Pontillo A. Variants in NLRP3 and NLRC4 inflammasome associate with susceptibility and severity of multiple sclerosis. Mult Scler Relat Disord. 2019;29:26-34.

73.   Hiruma J, Harada K, Motoyama A, Okubo Y, Maeda T, Yamamoto M, et al. Key component of inflammasome, NLRC4, was identified in the lesional epidermis of psoriatic patients. J Dermatol. 2018;45(8):971-7.

74.   Wang J, Ye Q, Zheng W, Yu X, Luo F, Fang R, et al. Low-ratio somatic NLRC4 mutation causes late-onset autoinflammatory disease. Annals of the rheumatic diseases. 2022.

75.   Li B, Dewey CN. RSEM: accurate transcript quantification from RNA-Seq data with or without a reference genome. BMC bioinformatics. 2011;12:323.

76.   Zhou G, Soufan O, Ewald J, Hancock REW, Basu N, Xia J. NetworkAnalyst 3.0: a visual analytics platform for comprehensive gene expression profiling and meta-analysis. Nucleic acids research. 2019;47(W1):W234-W41.

Figure 1

A
Impact of treatment duration on clinical parameters

B

C

D

Figure 1. Alterations in frequencies and expression of CD64 in dendritic cell subsets present in peripheral blood and synovial fluid from RA patients. (A-B): Analysis of DAS28-ESR and number of swollen joint count (SJC) (A) or proportions of CD1c^{+} cDCs (B) in blood samples from n=31 RA patients collected at the first visit (untreated baseline) and after 1 or 2 years of treatment. Statistical significance was calculated using a two-tailed matched pairs Wilcoxon test. (C): Proportions of CD40 (left), and CD64 (center) and CD16 (right) on gated CD1c^{+} cDC (upper plots) and CD141^{+} cDCs (lower plots) from the blood of healthy controls (HC, n=28) and untreated RA (n=31) patients and SF from treated RA patients (n=12). Statistical significance was calculated using a Kruskal Wallis test with Dunn´s correction. (D): Proportions of CD64^{+} cells within circulating CD1c^{+} cDC from the blood of n=19 HC and n=14 RA patients at baseline and 1-2 years after treatment initiation. Statistical significance was calculated using a two tailed-Mann Whitney test.

Figure 2

Figure 2. RNA-seq analysis of differential transcriptional signatures in circulating and synovial Mo, CD1c+ and CD141+ cDC from RA patients. (A): Number of individual (left) and overlapping (center, Venn's diagram) significant differentially expressed genes (DEG p<0.05 after FDR correction considering a Log2FC >1.5 and <-1.5) between circulating Mo, CD1c+ and CD141+ cDCs from n=4 untreated RA patients compared to n=4 healthy controls (HC). (B): Significance of selected upregulated (positive z-score; red), downregulated (negative z-score; blue) or undetermined (0 or not predicted Z-score; grey) canonical pathways predicted by Ingenuity Pathway Analysis (IPA) (full analysis shown in Supplemental Table 5) for DEG from Mo, CD1c+ cDCs and CD141+ cDCs from RA vs HC. *p<0.05; **p<0.001; ***p<0.0001. (C): Circos plot analyzing level of connection and shared genes between some of the pathways significantly altered in CD1c+ cDCs from the blood of RA patients shown in panel B. Genes within each pathway are ordered according to upregulated (red scale) and downregulated (blue scale) transcriptional levels. Quantification of interactions between pathways in the circos plot is illustrated on the heatmap shown on the right. (D): Venn's diagram of overlapping significant DEG in CD1c+ cDCs from the blood and synovial fluid (SF) from RA individuals compared to healthy controls (HC) or Calcium Pyrophosphate Deposition (CPPD) crystal-associated arthropathy patients. (E): Significance of selected pathways for 73 overlapping DEG and 905 non-overlapping DEG in CD1c+ cDC from SF mentioned in (D) predicted by DAVID.

Figure 3

Figure 3. Expression of CCR2 on CD1c+ cDCs associates with depletion of CD64Hi activated cells from the blood of RA patients.
(A-C): Heatmaps reflecting Log2(FC) in the transcription of inflammatory cytokines downstream TLR and inflammasome (A) or the indicated chemokine receptors (C) in circulating CD1c+ cDCs (blue bars), CD141+ cDCs (red bars) and Mo (cyan bars) from peripheral blood (PB) of n=4 RA patients versus n=4 healthy controls. Size of yellow circles represent different levels of statistical significance. (B): RT-qPCR analysis of expression of some of the cytokines identified in (A) relative to β-Actin levels in PB CD1c+ cDC (upper plots) and Mo (lower plots) from n=4 healthy controls (blue, HC) compared to n=5 RA patients (magenta). (D): Proportions of total CCR2Hi cells included in the CD1c+ cDC from the blood of n=20 RA patients (magenta) and n=17 HC (blue). Statistical significance was calculated using a two tailed Mann Whitney Test. **p<0.01. (E): Proportions of CD64+ cells present on gated CCR2Lo or CCR2Hi subpopulations of CD1c+ cDC from the blood of RA patients. (F): Proportions of CCR2+ cell from synovial fluid (SF) Mo and CD1c+ and CD141+ cDCs from RA (n=4, red) patients. Data represent mean and SEM values.
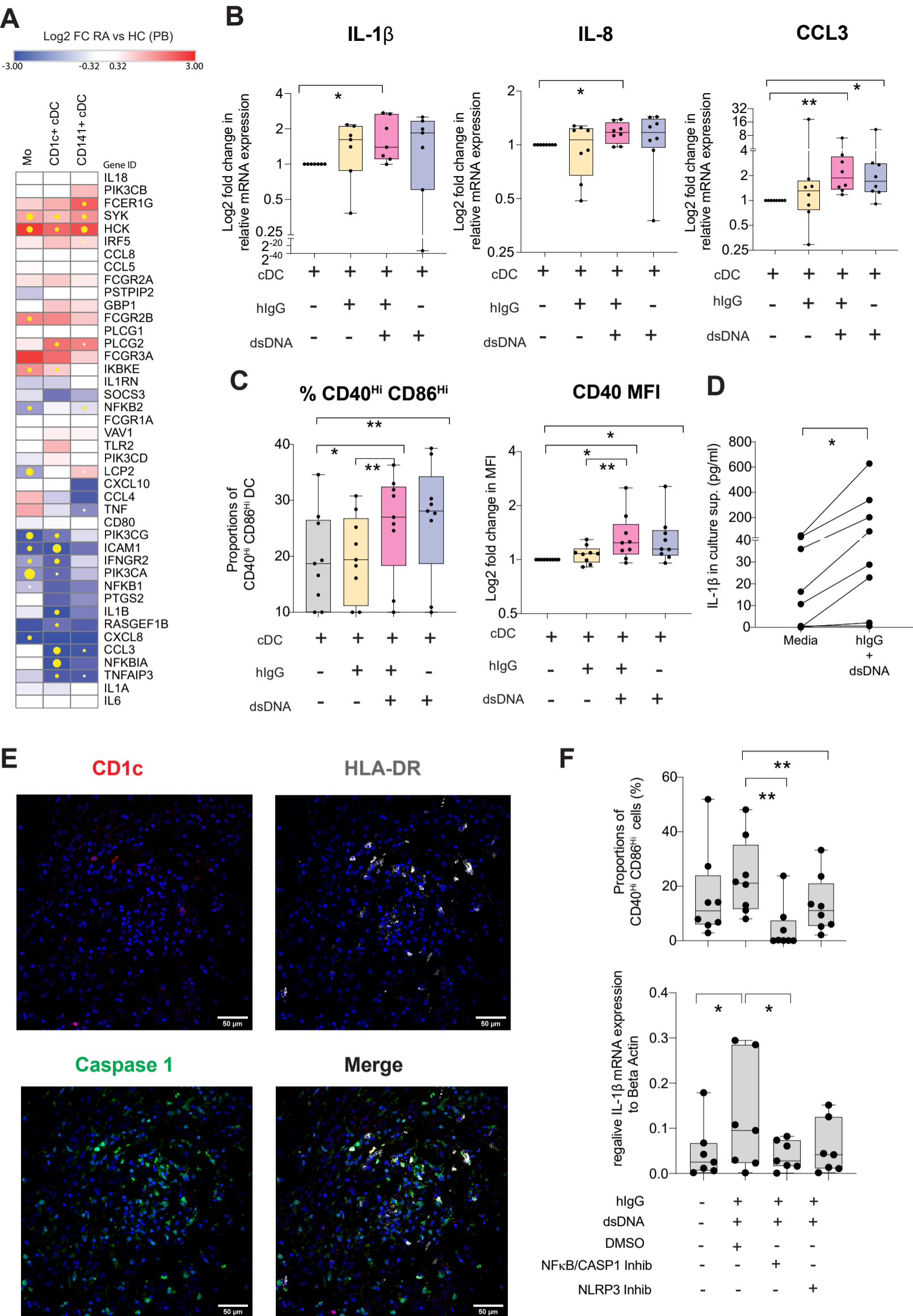
Figure 4
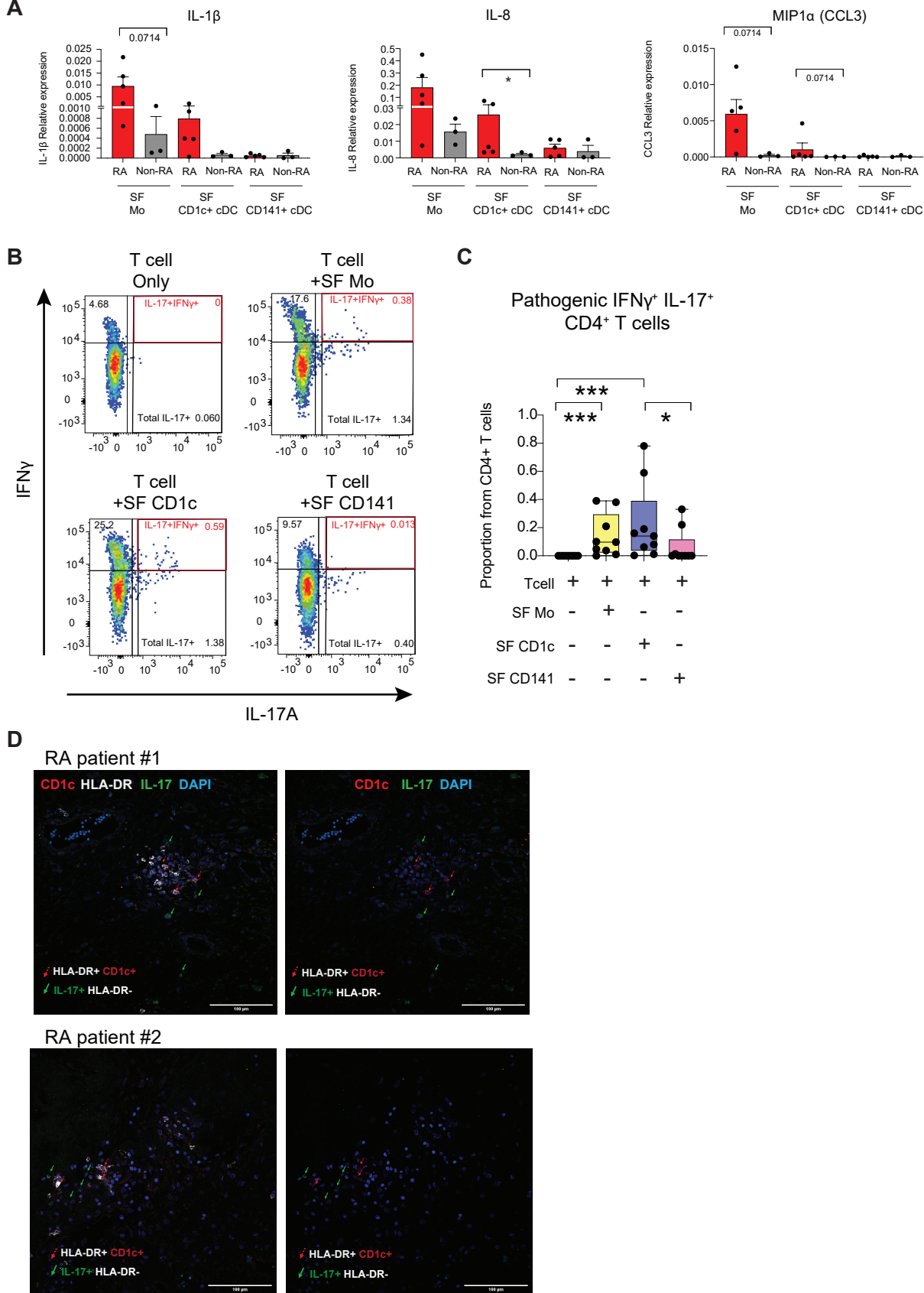
Figure 4. Inflammatory and functional profiles in circulating and synovial CD1c+ cDCs from RA patients. (A): RT-qPCR analysis of the indicated cytokines relative to β-Actin levels in sorted populations from RA (n=5) and CPPD-associated arthropathy (n=3) synovial fluids (SF). (B): Representative FACS analysis of IFNγ vs IL-17a expression on CD4+ T cells cultured for 5 days alone or in the presence of Mo, CD1c+ and CD141+ cDCs from the SF of RA patients. Proportions of total IL17+ and pathogenic IL-17a+ IFNγ+ CD4+ T cells are highlighted in black and red gates, respectively (C): Quantification of proportions of pathogenic IL-17a+ IFNγ+ CD4+ T cells induced under the conditions defined in (B), from n=9 HC. Statistical significance was calculated using two-tailed Wilcoxon matched pairs signed rank test (*p<0.05; **p<0.01). (D): Representative confocal microscopy images (original magnification 40X) showing infiltrated HLA-DR+ CD1c+ cells and IL-17+ cells in close proximity in histological sections of synovial membrane from n=6 RA patients. Images showing co-expression with HLA-DR or without this marker are shown on the left and right, respectively.
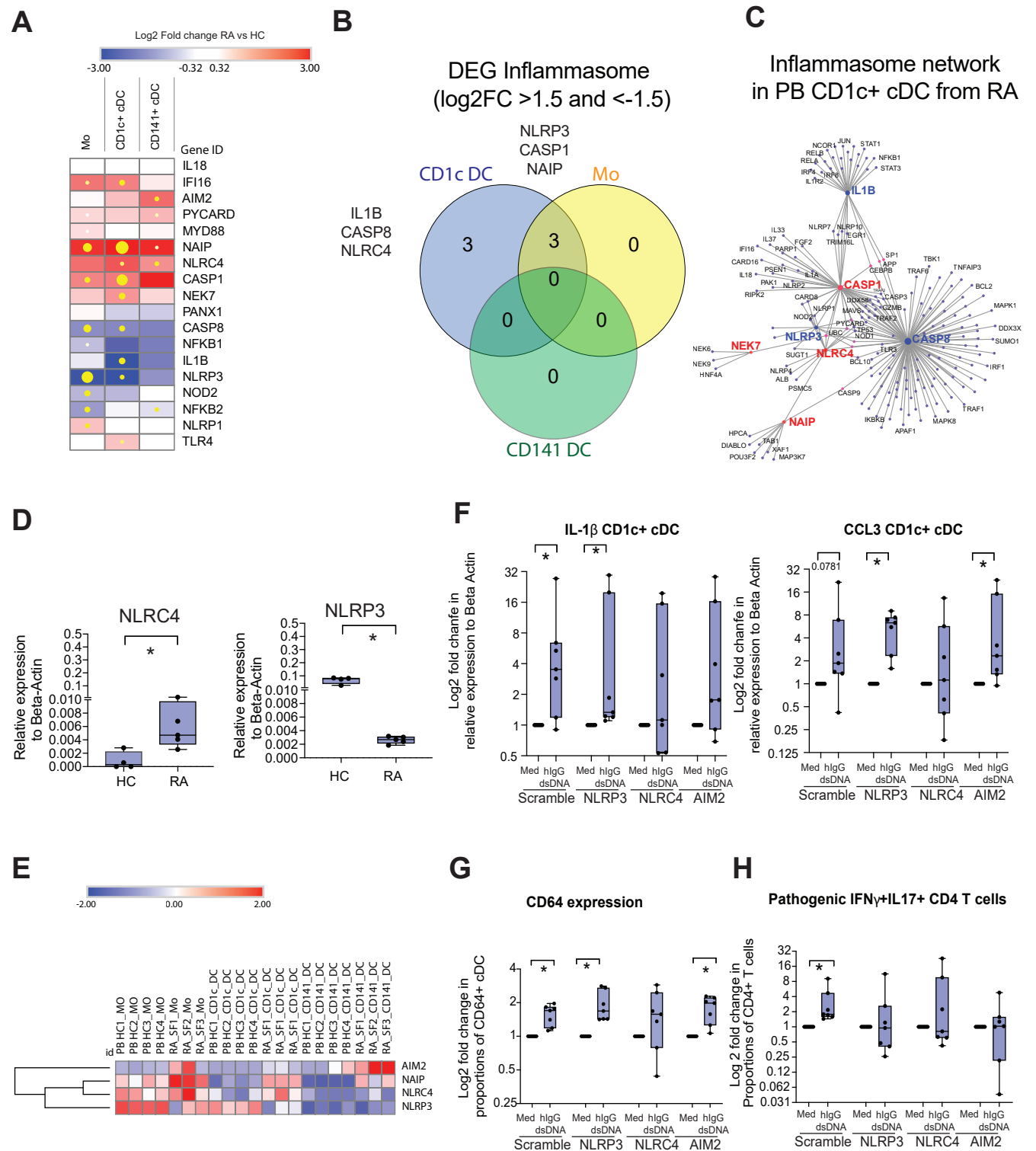
Figure 5

A
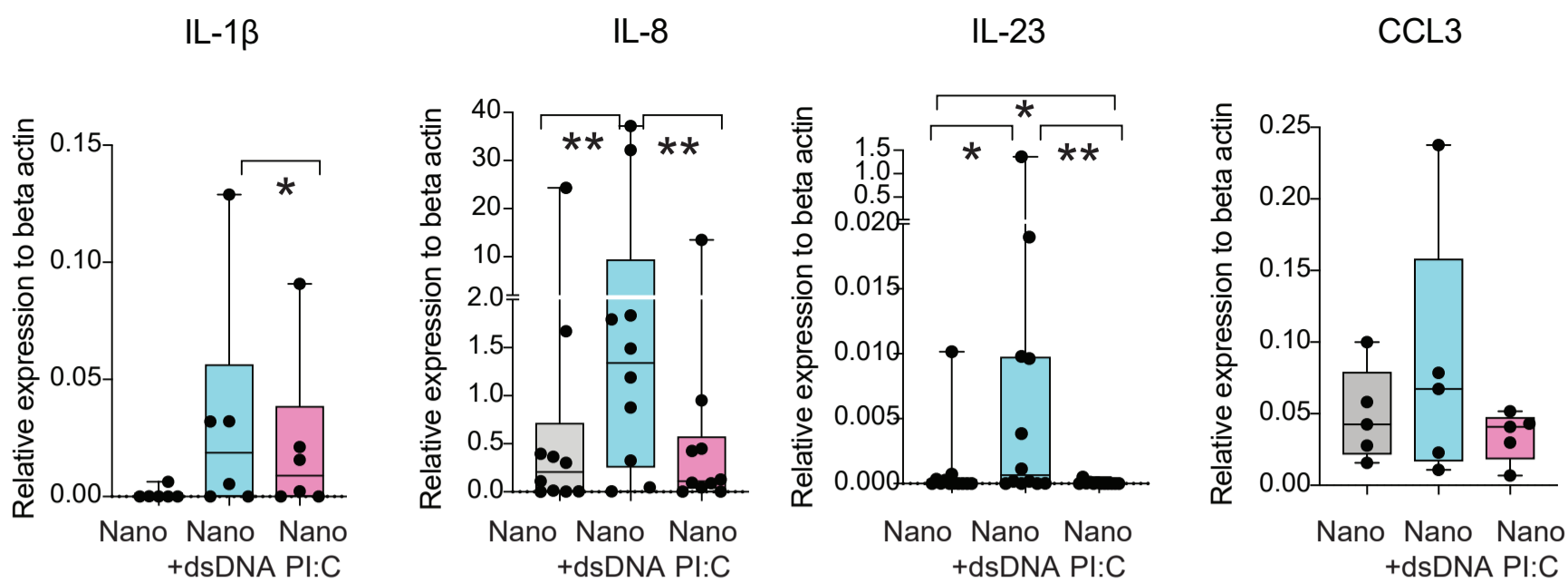
B
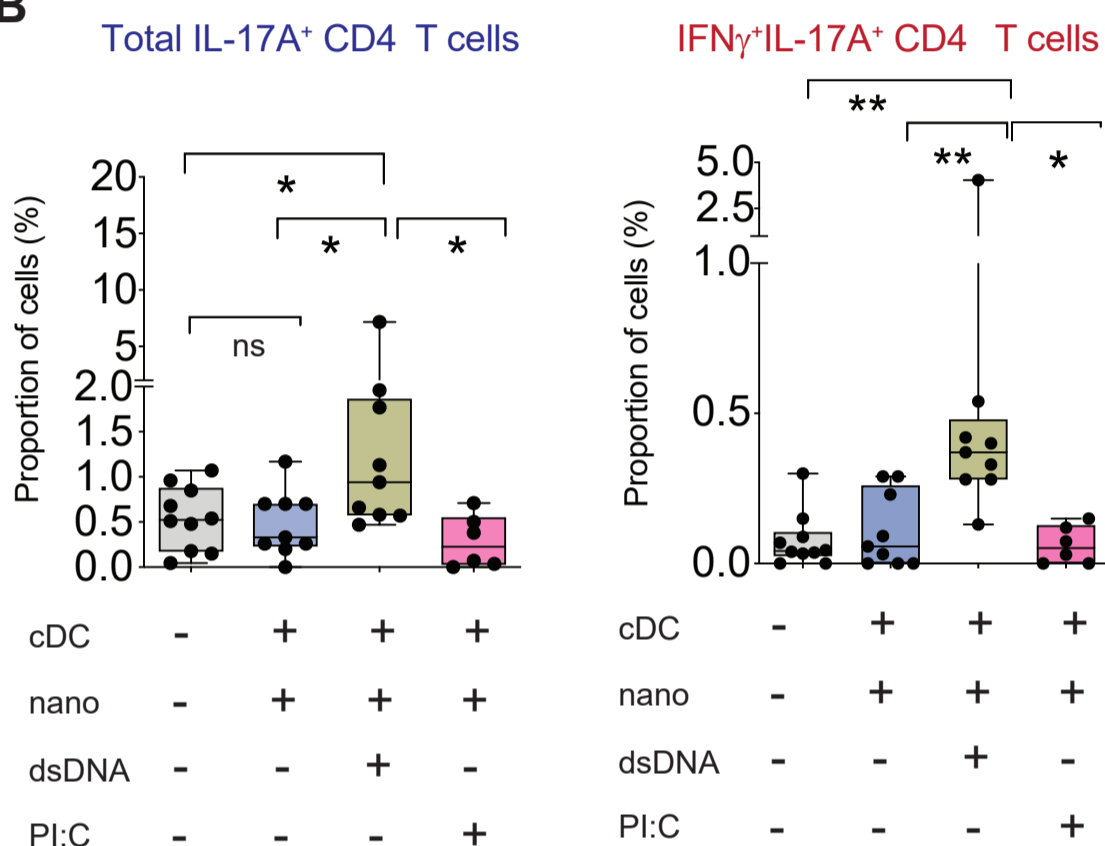
C
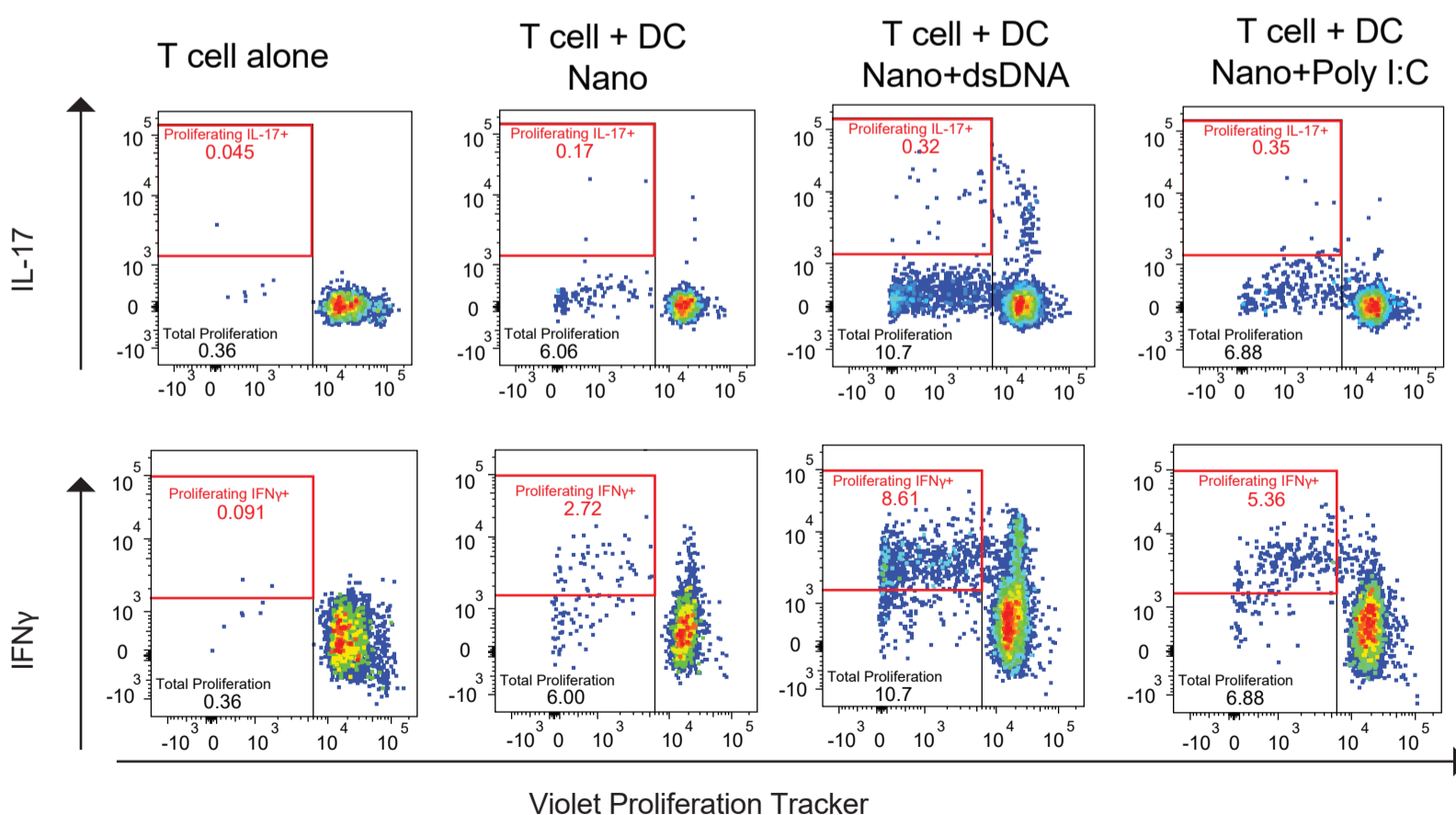
Figure 5. Intracellular dsDNA induces RA-like inflammatory cytokine profile and Th17-stimulating function on CD1c⁺ cDCs. (A): RT-qPCR analysis of mRNA levels of IL-1β (n=6), IL-8 (n=10), IL-23 (n=12), and CCL3 (MIP1α; n=5) relative to β-Actin in primary CD1c⁺ cDCs after 24h of culture in the presence of media and with empty nanoparticles (Nano) or nanoparticles loaded with dsDNA (Nano+dsD-NA) or Poly (I:C) (Nano+PI:C). Statistical significance was calculated using a two-tailed Wilcoxon matched-pairs test. *p<0.05; **p<0.0.1 (B): Analysis of frequencies of total IL-17⁺ (left) and IFNγ⁺ IL-17⁺ (right) CD4+ T cells cultured for 5-6 days alone or in the presence of allogeneic primary circulating CD1c⁺ cDCs pre-stimulated as previously mentioned at a T:DC ratio 1:1 (n=9). Statistical significance was calculated using a two-tailed Wilcoxon matched pairs test. *p<0.05; **p<0.01. (C): Representative FACS dot plots showing levels of Violet Proliferation Tracker vs expression of IL-17 (upper plots) or IFNγ (lower plots) on CD4⁺ T cells present in the different culture conditions described in (A). Statistical significance was calculated using a two tailed Wilcoxon matched pairs test. *p<0.05.

Figure 6

Figure 6. Crosstalk of Fcγ-R and inflammasome in CD1c+ cDC in response to dsDNA/IgG complexes. (A): Heatmaps reflecting log2FC in transcription of 42 genes associated with Fc-receptor signaling on sorted Mo, CD1c^{+} and CD141^{+} cDC from the peripheral blood (PB) of n=4 RA individuals compared to corresponding n=4 healthy controls. Significant DEG are highlighted in yellow (left heatmap, p<0.05 FDR) dots. Size of dots is proportional to significance level. (B): RT-qPCR analysis of expression of IL-1β (n=6), IL-8 and CCL3 (n=7) relative to β-Actin in circulating cDCs cultured for 24h in the presence of media or human IgG (hIgG) complexes alone (yellow bars) or in combination with dsDNA (pink bars) or media containing dsDNA (blue bars). *p<0.05; **p<0.01. (C): Proportions of CD40^{+} CD86[Hi] cDCs (left) and Mean of Fluorescence intensity (MFI) of CD40 on these cells (right) and analyzed by FACS in the experiments detailed in (B). *p<0.05; **p<0.01. (D): ELISA quantification of IL1-β on culture supernatants of CD1c^{+} cDC exposed to Media or hIgG-dsDNA complexes for 24h. Significance was calculated using a two-tailed Wilcoxon pairs-matched test. (E): Representative confocal microscopy image (magnification 40X) analyzing expression of Caspase 1, CD1c and HLA-DR on histological sections from inflamed synovial membrane from a representative RA patient from n=3 individuals tested. (F): Proportions of CD40[Hi] CD86[Hi] cDCs cultured in media alone or activated with Ig-dsDNA complexes in the presence or either DMSO, or a Caspase 1/NFκB inhibitor or a NLRP3 inhibitor (n=8 experiments). Statistical significance was calculated using a two-tailed Wilcoxon test. **p<0.01.

Figure 7

Figure 7. Identification of NLRC4 as the sensor potentially driving pathogenic activation of CD1c⁺ cDC in RA patients. (A): Heatmap representing log2-FC in transcription of 18 inflammasome genes on each sorted myeloid cell subset from the peripheral blood (PB) from n=4 RA *vs* n=4 healthy controls (HC) (red, upregulated; blue, downregulated). Yellow dots size is proportional to statistical significance between PB RA and healthy donors (p<0.05 FDR p values). (B): Venn´s diagram showing overlap of DEG associated with the inflammasome by IPA in the indicated myeloid cell subsets from the blood of n=4 RA patients compared to n=4 healthy donors. (C): Gene network including significantly upregulated (red) or downregulated (blue) DEG inflammasome genes in PB CD1c⁺ cDCs from RA patients compared to HC (right). Individual (violet) and connected target genes (pink) are shown. (D): mRNA expression of NLRC4 (left plot) and NLRP3 (right plot) relative to β-Actin validated by qPCR in sorted CD1c⁺ cDC from n=5 RA patients and n=4 HC individuals. Statistical significance was calculated with a two tailed Mann Whitney test. *p<0.05 (E): Unsupervised heatmap reflecting normalized expression levels of the indicated inflammasome sensors in Mo, CD1c⁺ cDC and CD141⁺ cDC from n=3 SF of RA patients versus the same myeloid subsets from the blood of n=4 HC. (F-G-H): Fold change on IL-1β and CCL3 mRNA expression relative to β-Actin mRNA levels analyzed by RT-qPCR (F), on surface expression of CD64 (G) and on functional ability to induce pathogenic IFNγ⁺ IL-17⁺ cells (H) in CD1c⁺ cDCs nucleofected with indicated siRNAs and cultured in media or in the presence of IgG-dsDNA complexes (n=7 experiments). Statistical significance was calculated using a two-tailed Wilcoxon matched-pairs test. *p<0.05.